UNCLASSIFIED

AD NUMBER

ADB011676

LIMITATION CHANGES

TO:

Approved for public release; distribution is unlimited.

FROM:

Distribution authorized to U.S. Gov't. agencies only; Administrative/Operational Use; SEP 1975. Other requests shall be referred to Air Force Avionics Laboratory, Wright-Patterson AFB, OH 45433.

AUTHORITY

AFAL ltr, 23 Mar 1979

THIS PAGE IS UNCLASSIFIED

THIS REPORT HAS BEEN DELIMITED
AND CLEARED FOR PUBLIC RELEASE
UNDER DOD DIRECTIVE 5200.20 AND
NO RESTRICTIONS ARE IMPOSED UPON
ITS USE AND DISCLOSURE.

DISTRIBUTION STATEMENT A

APPROVED FOR PUBLIC RELEASE;
DISTRIBUTION UNLIMITED.

AFAL-TR-75-172

EFFECTS OF VIBRATION AND G LOADING ON AIRBORNE E-O SENSOR AUGMENTED OBSERVERS

WESTINGHOUSE DEFENSE AND ELECTRONIC SYSTEMS CENTER
SYSTEMS DEVELOPMENT DIVISION
BALTIMORE, MARYLAND 21203

DDC
RECEIVED
JUN 15 1976
C

APRIL 1976

TECHNICAL REPORT AFAL-TR-75-172
FINAL REPORT FOR PERIOD 2 FEBRUARY 1975 - 30 MAY 1975

AD No. ADB011676
DDC FILE COPY

DISTRIBUTION LIMITED TO U. S. GOVERNMENT AGENCIES ONLY; TEST AND EVALUATION; SEPTEMBER 1975. OTHER REQUESTS FOR THIS DOCUMENT MUST BE REFERRED TO AFAL/RWI.

AIR FORCE AVIONICS LABORATORY
AIR FORCE WRIGHT AERONAUTICAL LABORATORIES
AIR FORCE SYSTEMS COMMAND
WRIGHT-PATTERSON AFB, OHIO

NOTICE

When Government drawings, specifications, or other data are used for any purpose other than in connection with a definitely related Government procurement operation, the United States Government thereby incurs no responsibility nor any obligation whatsoever; and the fact that the government may have formulated, furnished, or in any way supplied the said drawings, specifications, or other data, is not to be regarded by implication or otherwise as in any manner licensing the holder or any other person or corporation, or conveying any rights or permission to manufacture, use, or sell any patented invention that may in any way be related thereto.

This technical report has been reviewed and is approved for publication.

Frederick P. Blommel

FREDERICK P. BLOMMEL
Project Engineer

R. E. Deal

ROBERT E. DEAL, Chief
Electro-Optics & Reconnaissance Branch
Reconnaissance & Weapon Delivery Division

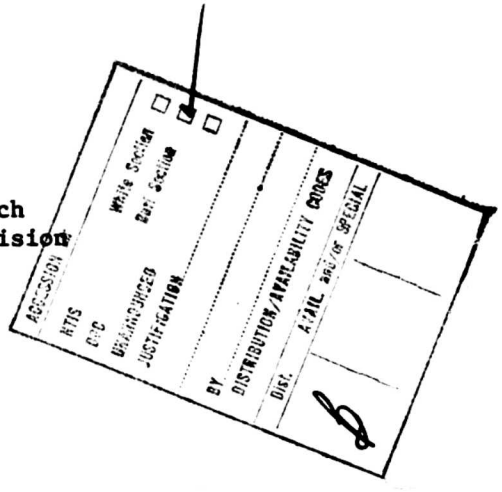

Copies of this report should not be returned unless return is required by security considerations, contractual obligations, or notice on a specific document.

UNCLASSIFIED

SECURITY CLASSIFICATION OF THIS PAGE (When Data Entered)

REPORT DOCUMENTATION PAGE

READ INSTRUCTIONS BEFORE COMPLETING FORM

1. REPORT NUMBER	2. GOVT ACCESSION NO.	3. RECIPIENT'S CATALOG NUMBER
AFAL-TR-75-172		

4. TITLE (and Subtitle)
EFFECTS OF VIBRATION AND G LOADING ON AIRBORNE SENSOR AUGMENTED OBSERVERS

5. TYPE OF REPORT & PERIOD COVERED
Final 2 Feb 1975 - 30 May 1975

6. PERFORMING ORG. REPORT NUMBER

7. AUTHOR(s)
Robert H. Willson
Frederick A. Rosell
Heru Ra Walmsley

8. CONTRACT OR GRANT NUMBER(s)
F33615-75-C-1067

9. PERFORMING ORGANIZATION NAME AND ADDRESS
Westinghouse Defense and Electronic Systems Center, Systems Development Division, Baltimore, Maryland

10. PROGRAM ELEMENT, PROJECT, TASK AREA & WORK UNIT NUMBERS
PE 62204F; Project 2004, Task 02, Work Unit 06

11. CONTROLLING OFFICE NAME AND ADDRESS
Air Force Avionics Laboratory, Air Force Systems Command, United States Air Force, Wright-Patterson AFB, Ohio

12. REPORT DATE
APR 1976

13. NUMBER OF PAGES
82

14. MONITORING AGENCY NAME & ADDRESS (if different from Controlling Office)
Final rept. 2 Feb - 30 May 75

15. SECURITY CLASS. (of this report)
UNCLASSIFIED

15a. DECLASSIFICATION/DOWNGRADING SCHEDULE

16. DISTRIBUTION STATEMENT (of this Report)
Distribution limited to U. S. Government Agencies only; Test and Evaluation; September 1975. Other requests for this document must be referred to AFAL/RWI.

89p.

17. DISTRIBUTION STATEMENT (of the abstract entered in Block 20, if different from Report)
AF-2004

200402

18. SUPPLEMENTARY NOTES

19. KEY WORDS (Continue on reverse side if necessary and identify by block number)
vision, vibration and g effects on observers, visual thresholds, detection and recognition performance, airborne television systems

20. ABSTRACT (Continue on reverse side if necessary and identify by block number)
Psychophysical experiments were performed to quantitatively determine the effect of vibration and g loading on the ability of observers to perform certain visual tasks in a realistic flight environment. The test aircraft used was a corporately owned Sabreliner. The performance of four observers was measured on the ground, in straight and level flight, under conditions of moderate-to-severe turbulence and under conditions of sustained g loading. The test images were televised squares and bar patterns to which white noise of

OVER

DD FORM 1 JAN 73 1473 EDITION OF 1 NOV 65 IS OBSOLETE

UNCLASSIFIED 405 897

SECURITY CLASSIFICATION OF THIS PAGE (When Data Entered)

LB

20. Abstract (continued)

various amounts were added. It was found that the observers were unaffected by straight and level flight, were not appreciably affected by g loading but were moderately affected by turbulence.

PREFACE

This report was prepared by the Systems Development Division of Westinghouse Defense and Electronics Systems Center. The program manager was Marvin Tenberg. He was assisted in the program and report preparation by Robert Willson, Frederick Rosell, and Heru Walmsley. The project engineer was Frederick Blommel, Air Force Avionics Laboratory, Wright-Patterson AFB, Ohio.

TABLE OF CONTENTS

Section		Page
1.0	INTRODUCTION	1
2.0	EXPERIMENTAL SET-UP, EQUIPMENT INSTALLATION ...	7
2.1	Aircraft	7
2.2	Equipment Installation	7
3.0	RECTANGULAR IMAGES	13
3.1	Historical Background	13
3.2	Experimental Procedure	20
3.3	Analysis of Data	28
3.4	Operator Comments	37
4.0	BAR PATTERN IMAGES	39
4.1	Historical Background	39
4.2	Experimental Procedure	44
4.3	Analysis of Data	45
4.4	Operator Comments	60
4.5	Vibration Data	60
5.0	RECOMMENDED FOLLOW-ON EFFORTS	63
APPENDIX A.	SUMMARY REPORT MOTION ANALYSIS FLIR/ACTV AIRBORNE OPERATOR TEST PROGRAM	65

LIST OF ILLUSTRATIONS

Figure		Page
1	Experimenter's Equipment	8
2	Observer Compartment	9
3	Airborne Operator Test Equipment Setup	10
4	The Display Signal-to-Noise Ratio Experiment ...	14
5	Probability of Detection vs Video Signal-to-Noise Ratio Required for Rectangular Images of Size ○ 4 x 4, □ 4 x 64, △ 4 x 128, and ◇ 4 x 180 Scan Lines. Televised Images at 30 Frames per Second. Observer-to-Display Viewing Distance/Display Height (D_V/D_H) = 3.5.....	16
6	Corrected Probability of Detection vs SNR_D Required for Rectangular Images of Size ○ 4 x 4, □ 4 x 64, △ 4 x 128, and ◇ 4 x 180 Scan Lines. Televised Images at 30 Frames per Second and 525 Scan Lines. D_V/D_H = 3.5.....	17
7	Probability of Detection vs SNR_D for Squares of Various Size at a Display Distance to Height Ratio of 3.5.....	17
8	Threshold Signal-to-Noise Ratio vs Size of Square in Scan Lines. D_V/D_H = 3.5.....	18
9	Layout of Observer's Compartment	21
10	Angular Subtense of 2 x 2 Square at the Observer's Eye as a Function of Viewing Distance for Various Display Diagonal Dimensions.....	21
11	Threshold SNR_{DT} as a Function of Square Size for (○) Straight and Level Flight, and (●) Lab Conditions.....	29

LIST OF ILLUSTRATIONS

(continued)

Figure		Page
12	Threshold SNR_{D-T} as a Function of Square Size for Straight and Level Flight after 2½ g turns and ± 0.4 g Turbulence, Flight No. 2.....	30
13	Threshold SNR_{D-T} as a Function of Square Size for Straight and Level Flight for Two Flights. ○ Flight #1 Data and □ Rescaled Data from Flight #2.....	31
14	Threshold SNR_{D-T} as a Function of Square Size for ± 0.2 g, 1 sec Period Turbulence, ○ Flight No. 3 Data and ● Average Straight and Level Data.....	32
15	Threshold SNR_{D-T} as a Function of Square Size for ± 0.35 g, 2 sec Period Turbulence. ○ Flight No. 4 Data, ◇ Average Straight and Level Flight and ● Rescaled Data for Turbulent Conditions.....	34
16	Threshold SNR_{D-T} as a Function of Square Size for the Four Flights and Lab Comparison Data; ● Lab, ○ Straight and Level Flight No. 1, □ Straight and Level Flight No. 2 (Scaled), ◇ Turbulent Flight No. 3, ◆ Turbulent Flight No. 4 (Scaled).....	35
17	Ratio Between Threshold SNR_{D-T} for Squares for Average of Straight and Level, and Lab Data to the Average Data for Turbulent Conditions.....	36
18	Experimental Setup for Television Camera Generated Imagery	40
19	Fraction of Bar Patterns Resolved vs Display Signal-to-Noise Ratio for a 396-Line Bar Pattern of Length-to-Width Ratio □ 5:1, ○ 10:1, ● 20:1 Televised Images at 25 Frames/Sec. 875 Scan Lines, D_V/D_H = 3.5.....	41
20	Threshold Display Signal-to-Noise Ratio vs Bar Pattern Spatial Frequency for Three Bar Length-to-Width Ratios of □ 5:1, ○ 10:1, ● 20:1 Televised Images at 25 Frames/Sec. 875 Scan Lines, D_V/D_H = 3.5.....	41

LIST OF ILLUSTRATIONS

(continued)

Figure		Page
21	Fraction of Bar Patterns Resolved vs Display Signal-to-Noise Ratio for Bar Patterns of Spatial Frequency ○ 104, ● 200, □ 329, ■ 396, ◇ 482 and ◆ 635 Lines per Picture Height. Bar Height-to-Width Ratio was 5 in All Cases. Televised Images at 25 Frames/Sec. 875 Scan Lines, D_V/D_H = 3.5.....	42
22	Threshold Display Signal-to-Noise Ratio vs Bar Pattern Spatial Frequency Obtained Using Two Different Experimental Techniques; ● Method of Limits and ○ Method of Random SNR Variation. Televised Images at 25 Frames/Sec. 875 Scan Lines, D_V/D_H = 3.5.....	42
23	Threshold Display Signal-to-Noise Ratio vs Bar Pattern Spatial Frequency for Display to Observer Viewing Distances of ○ 14", □ 28", and ● 56". Televised Images at 25 Frames/Sec and 875 Scan Lines.....	43
24	Threshold SNR_{D-T} for Bar Patterns of Constant Bar Length - ○ Average Lab Data and □ Data in Aircraft on Ground.....	51
25	Threshold SNR_{D-T} vs Spatial Frequency for Flight No. 5 - ○ Data Taken Early in Flight and □ Data Taken Late in Flight. All Data for Straight and Level Flight - Method of Limits Used.....	52
26	Threshold SNR_{D-T} vs Spatial Frequency for Flight No. 8 - ○ Data Taken Early in Flight and □ Data Taken Late in Flight. All Data for Straight and Level Conditions - Method of Random SNR Variation Used.....	53
27	Threshold SNR_{D-T} vs Spatial Frequency for ○ Flight No. 6 (Method of Limits Used) and □ Flight No. 7 (Method of Random SNR Variation Used) for Straight and Level Flight Conditions.....	54

LIST OF ILLUSTRATIONS

(continued)

Figure		Page
28	Average Threshold SNR_{D-T} for Bar Pattern Recognition Under Straight and Level Flight Conditions - $\pm$ 1 σ Limits (♦).....	56
29	Threshold SNR_{D-T} for Bar Pattern Recognition Under Turbulent Conditions - ○ Method of Limits Flight No. 6, □ Random SNR Variation Flight No. 7, and (———) Average.....	57
30	Ratio of SNR_{D-T} for Straight and Level Flight to the SNR_{D-T} for Turbulent Flight Conditions for Bar Pattern Recognition.....	58
31	Threshold SNR_{D-T} as a Function of Spatial Frequency During 2½ g Steep Turns for Bar Pattern Recognition, ○ Random SNR Flight No. 7; □ Method of Limits Flight Nos. 5, 6, 8; ◇ Random dB Flight No. 8; and (———) Composite Average.....	59
32	Composite Average Threshold SNR_{D-T} Data for Bar Pattern Recognition - ■ Aircraft on Ground, ◇ Straight and Level Flight, ◆ 2½ g Turns, and ● Turbulence.....	61
33	Elimination of Irregular Tape Record Speed Effects.....	73
34	Calm Flight Mode - Slow Paper Speed - Illustrating Overall Acceleration Levels (Flight No. 6).....	74
35	Rough Flight Mode - Slow Paper Speed - Illustrating Overall Acceleration Levels (Flight No. 6).....	75
36	Average Overall Acceleration Levels (Flight No. 6) Relative to Flight Time Log.....	76
37	Average Overall Acceleration Levels (Flight No. 7) Realtive to Flight Time Log.....	77
38	Calm Flight Mode - Fast Paper Speed - Illustrating Frequency Components of Motion (Flight No. 6).....	78

LIST OF ILLUSTRATIONS

(continued)

Figure		Page
39	Rough Flight Mode - Fast Paper Speed - Illustrating Frequency Components of Motion (Flight No. 6).....	79
40	Rough Flight Mode (Flight No. 7) - Average Acceleration Amplitude vs Amplitude vs Frequency - Channels 4, 5, 6, and 8.....	80
41	Rough Flight Mode (Flight No. 7) - Average Acceleration Amplitude vs Frequency - Channels 9, 10, 11, and 12.....	81
42	Calm Flight Mode (Flight No. 7) - Average Acceleration Amplitude vs Frequency - Channels 4 and 9.....	82

LIST OF TABLES

Table		Page
1	Threshold SNR_{DT} vs Square Size for Two Display Distance to Display Height Ratios.....	19
2	Rectangular Image Test.....	23
3	Typical Test Control Sheet.....	24
4	Typical Observer Test Sheet.....	25
5	Preflight Checklist.....	26
6	The Number of Data Points Taken Each Flight for Various Conditions for Squares.....	28
7	Experimenters Sheet.....	46
8	Observer Sheet.....	47
9	Summary of Data Collated for Bar Pattern Experiments.....	48
10	Observer Threshold SNR_{D-T} for Bar Pattern Recognition from Lab Data.....	50
11	Flight Test Channel Designation.....	72

1.0 INTRODUCTION

During the last decade, the use of airborne electro-optical sensors has greatly increased. Recently, the utility of electro-optical sensors on aircraft making high speed, low altitude penetrations into hostile territories has become the subject of extensive investigation. Under low altitude, high speed flight conditions, pilots and navigators become subject to severe vibration and, in weapon delivery and escape modes, may also be subject to high g loadings.

While many experiments have been performed to measure the effect of severe vibration and g loading on humans, an extensive review of the literature failed to find usable quantitative data with regard to the ability of observers to use electro-optically generated and displayed imagery under such stress conditions. Over the last few years, a substantial data base of observer visual thresholds has been established and reported in references 1 - 5. These thresholds were

---

1. Rosell, F. A., and Willson, R. H., Performance Synthesis (Electro-Optical Sensors) AFAL-TR-71-137, Air Force Avionics Laboratory, WPAFB, Ohio, May 1971.
2. Rosell, F. A., and Willson, R. H., Performance Synthesis (Electro-Optical Sensors) AFAL-TR-72-279, Air Force Avionics Laboratory, WPAFB, Ohio, August 1972, AD-905-291L.
3. Rosell, F. A., and Willson, R. H., Performance Synthesis of Electro-Optical Sensors, AFAL-TR-73-260, Air Force Avionics Laboratory, WPAFB, Ohio, August 1973.
4. Biberman, L. M., "Perception of Displayed Information," Plenum Press, New York, May 1973.
5. Rosell, F. A., and Willson, R. H., Performance Synthesis (Electro-Optical Sensors) AFAL-TR-74-104, Air Force Avionics Laboratory, WPAFB, Ohio, April 1974.

collected under laboratory conditions through psychophysical experimentation. To gain some insight into the effects of realistic vibration and g loading on observers, it appeared logical, as a first step, to repeat the laboratory oriented psychophysical experiments in a real flight environment. It can be readily appreciated that any psychophysical experiments are statistical in nature and many thousands of data points are needed to gain significance. Tactical combat aircraft are primarily of the one or two seat variety and obviously, a two-seat version is needed as a minimum to perform any experiments since someone must pilot. Data collection in a real tactical aircraft would be a very costly operation.

Fortunately, the Westinghouse Electric Corporation's Systems Development Division has a corporate North American Sabreliner which could be made available for experimentation of the type needed. The Sabreliner though developed for commercial passenger use, is sufficiently rugged to withstand rather violent environmental conditions and can carry 4 observers, a pilot and co-pilot in addition to an experiment conductor and the necessary experimental apparatus. Furthermore, the bulk of the psychophysical experimentation in the visionics area has been conducted by Westinghouse personnel leading to an overall economy of testing.

While cost-effectiveness of the Westinghouse approach to data collection in this vital area was clearly evident, the usual pitfalls developed. The original scheme was to video tape record each experiment but the video bandwidth limitations of inexpensive commercial tape recorders, in addition to their uncertain vibration toleration, would have limited the scope of the data taken. Thus, a "live" experiment was substituted requiring the need for an experiment conductor. A further difficulty evolved. In the original proposal, it was

thought that a simple mount for the displays and instrumentation adapted to an existing table and a luggage rack could be used. However, safety considerations precluded the minimal cost approach and the installation was upgraded to meet FAA requirements. A special table was constructed and bolted to the longitudinal aircraft structural members. A special luggage rack equipment was constructed and the total ensemble was certified to meet a 9 g loading requirement. In spite of these unforeseen difficulties, the cost objectives of the overall program were met.

Two types of images were employed; namely, isolated squares and periodic images which consisted of bursts of bar patterns. These images have two singular virtues; the images are analytically describable and have behind them, a wealth of experimental data with regard to their detectability.

In general, specially selected and trained observers were used. The visual thresholds of the observers were measured first in the laboratory, then in the aircraft on the ground, in flight and in some cases in the laboratory again. Four observers were used on each flight. The three flight conditions employed were (1) straight and level in relatively smooth air, (2) moderate to heavy turbulence and (3) 2½ g loads induced by a circular turn.

1.1 The Effect of Severe Flight Environment on the Detection of Isolated Aperiodic Images

A square on a uniform background is considered to be an isolated aperiodic object. An image of this sort might simulate a tank on a desert background. Consider the experiments which used squares.

It was found that straight and level flight conditions gave the same results as were obtained in the laboratory and in the aircraft on the ground. The effect of the g environment was found to be negligible for the most part but turbulence did adversely affect observer thresholds having the most serious effects on the smallest squares as expected. However, the effect of turbulence was not severe - thresholds increased by

only about 25 to 50%. Surprisingly, rough air turbulence had a greater effect on the detection of squares than on periodic images.

1.2 The Effect of Severe Flight Environments on the Detection of Bar Patterns

Bar patterns were considered to be a more sensitive test of the effects of a severe flight environment. The bar patterns which were used were vertically oriented and ranged in spatial frequency from 100 to 800 lines/picture height but the MTF of the display coupled to the observer-to-display viewing distance precluded taking data beyond about 600 lines/picture height.

Surprisingly and unexpectedly, the observer thresholds measured in the aircraft on the ground were somewhat higher than measured in the laboratory. The effect, while small, was nevertheless real and as yet, unaccounted for. Using the in-aircraft measurements of bar pattern detectability as a baseline it was found that bar pattern detectability did not suffer under straight and level flight conditions nor did the 2½ g environment have any realistic perceptible effect.

As in the case of the detection of squares, it was found that turbulence was much more a problem than g loading but again, the effects were not large (less than a factor of 2 with respect to threshold SNR).

1.3 Observer Comments

The rough air environment simulated in the Sabreliner was thought to be similar to that encountered in an F-4 aircraft by the experienced F-4 pilots and navigators used in the experiments. Observers did report that g loading did not have much effect on either the detection of squares or bar patterns which was found to be the case. Turbulence was reported to be a more significant problem and was. One, not surprising outcome of the program, is that observer opinions cannot always be relied upon as an

indicator of real performance. While the observers thought fatigue was a problem, the data does not support this contention. Bar pattern detectability was measured using the method of limits and the method of random SNR variation. The observers thought that the method of limits was a much easier test but the experimental evidence does not bear them out.

2.0 EXPERIMENTAL SET-UP, EQUIPMENT INSTALLATION

The following paragraphs will deal with the relevant performance capabilities of the aircraft used in the experimental program and the equipment installation.

2.1 Aircraft

The aircraft which was used in the experiment was a North American jet NA-265 Sabreliner which is capable of simulating some of the in-flight environments of high performance aircraft such as F-4's. Eight flights were flown during the program and data was taken under three different conditions; (1) straight and level, (2) steep turns which pulled 2½ g's, and (3) rough air. Altitudes ranged from 2,500 feet to 28,000 feet and speeds ranged from 200 kts. to 450 kts. The rough air was found by flying at low altitudes between mountain ridges under cumulus cloud decks to closely approximate the "cobblestone effect" of turbulence during high speed target runs in F-4's. Two and one-half g steep turns (left and right) simulated moderate "jinking" maneuvers and steep turns over a target area. The total flight time for the program was slightly more than 14 hours of which about 10 hours were devoted to data taking.

2.2 Equipment Installation

The experimental setup in the aircraft is shown in Figs. 1 and 2. The experimenter and most of his equipment was in the baggage compartment between the pilot's cockpit and the cabin area. The experimenter's equipment is shown in Fig. 1 and a view of the observer compartment is shown in Fig. 2. Each equipment will be discussed briefly below. A block diagram of the interconnection of the equipment is shown in Fig. 3.

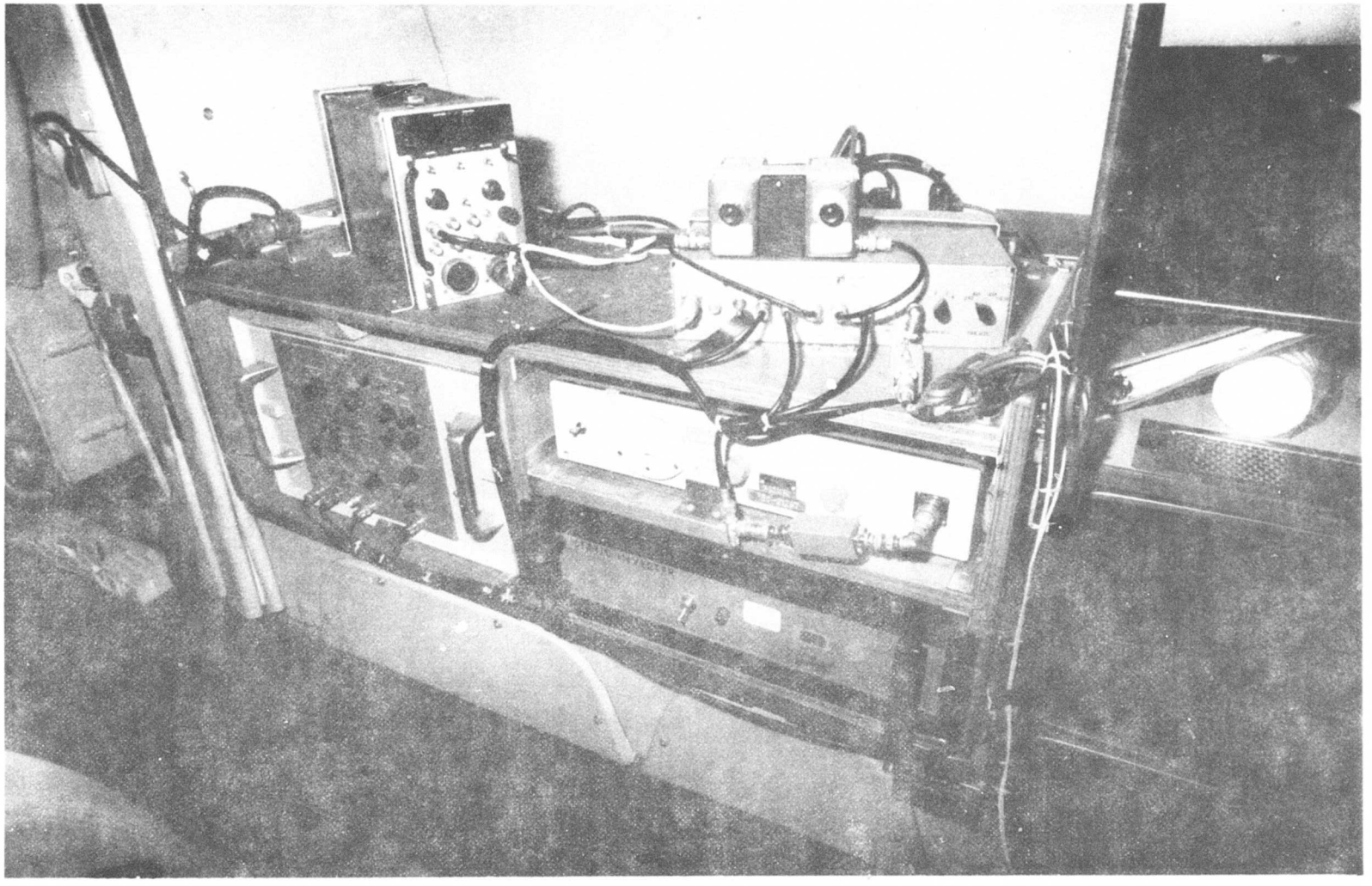

Figure 1 Experimenter's Equipment

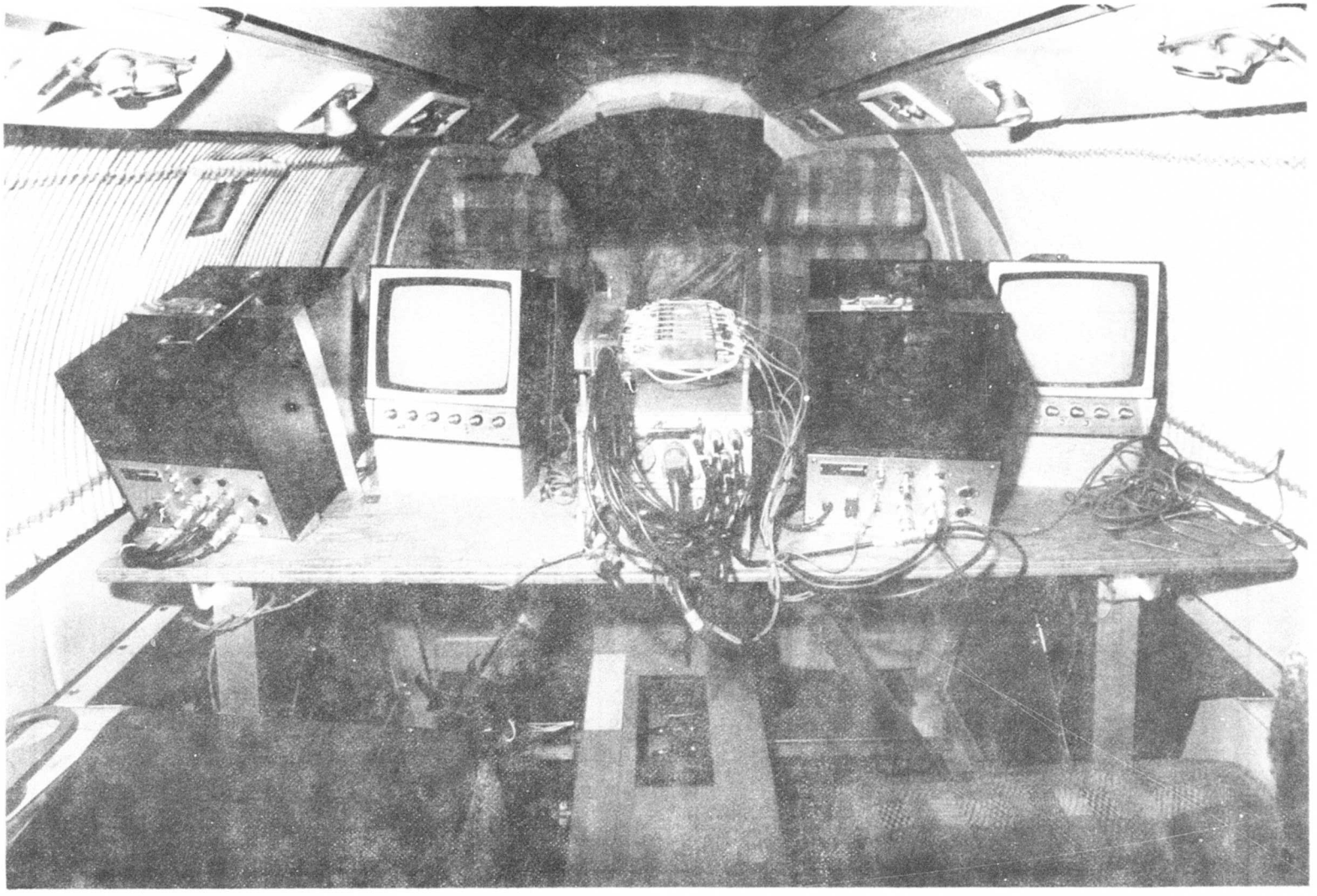

Figure 2 Observer Compartment

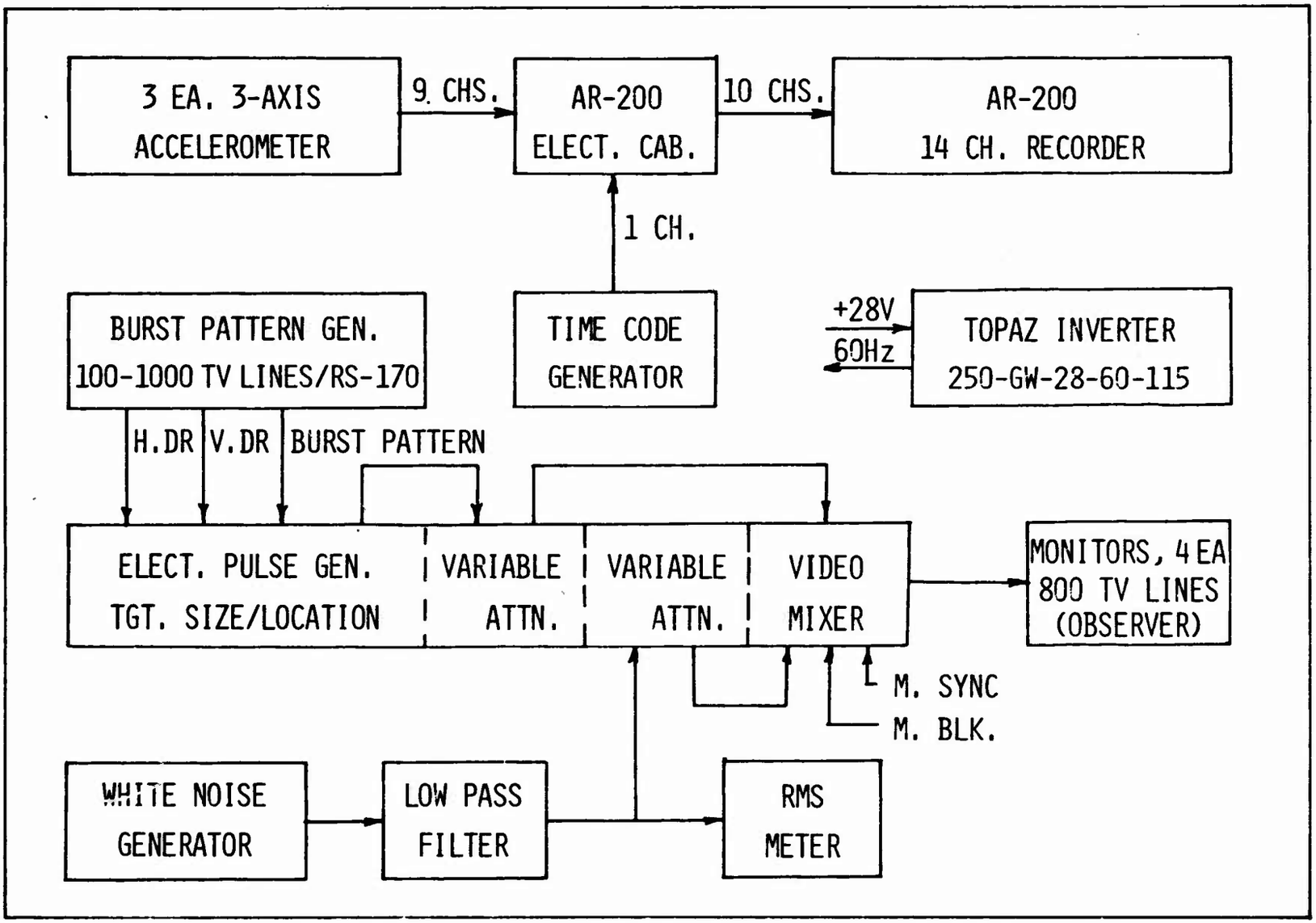

Figure 3 Airborne Operator Test Equipment Setup

Referring to Fig. 1, the upper left-hand portion of the photograph shows the time code generator for the accelerometers and directly below is the bar pattern (burst pattern) generator. In the upper right-hand portion is the square pattern generator and below is the noise generator and then the Topez power converter. In the cabin, there was room for four observers and four were tested at a time during each flight. Each observer had his own monitor. On the near left-hand seat is a 3-axis accelerometer board which the observer sat on and which is used to measure the acceleration loading on the observer. Two such seats were used at diagonally opposite positions. A 3-axis accelerometer was also mounted on the table. Below the table is the data recorder for the accelerometers and in the middle of the table is the accelerometer electronics. An accelerometer was also located in the aircraft cockpit.

A diagram of the experimental setup is shown in Fig. 3 and is the same in all important details as that used for the standard observer tests performed under previous Air Force 698DF Performance Synthesis programs. That is, known video signals and noise are mixed and added to the television monitors. The setup allows one to accurately control the signal to noise ratio of the signals to the monitors.

The observers view Panasonic TN-95/952 deluxe studio monitors. Maximum center resolution is 800 lines at 10 MHz bandwidth - a bandwidth adjustment allows the choice of 4 MHz, 8 MHz and 10 MHz video bandwidth. For the experiments with squares, the bandwidth was limited to 8 MHz while it was set at 10 MHz for the bar pattern experiments.

3.0 RECTANGULAR IMAGES

In this section, the experiments with rectangular images will be discussed. First, we will briefly discuss the historical background of the experiments with rectangles. Then, a discussion of the experimental procedure which was used in the aircraft will be presented. Finally, we will analyze the data and review the operator comments.

3.1 Historical Background

The earliest psychophysical experiments performed by Westinghouse on the 698DF program employed simple rectangular images on a uniform background. These images were electronically generated, mixed with additive white noise and displayed on a television monitor. The same amount of noise was added to both the rectangular image and its background. The purpose of the experiments was to determine the probability that an observer will detect a displayed image as a function of the image's signal-to-noise ratio. These experiments proved quite easy to perform and over the years, reruns of the experiment to establish equipment calibration have produced highly consistent results.

The basic experimental apparatus employed is shown schematically in Fig. 4. A signal pulse of rectangular waveform and variable duration is electronically generated and mixed with band-limited white noise of Guassian distribution. The spatial image displayed on the cathode ray tube (CRT) display is a rectangle which can appear in any of four quadrants (but always in the same position in the quadrant selected). The observer is asked to specify the quadrant in which the image is located as the video signal-to-

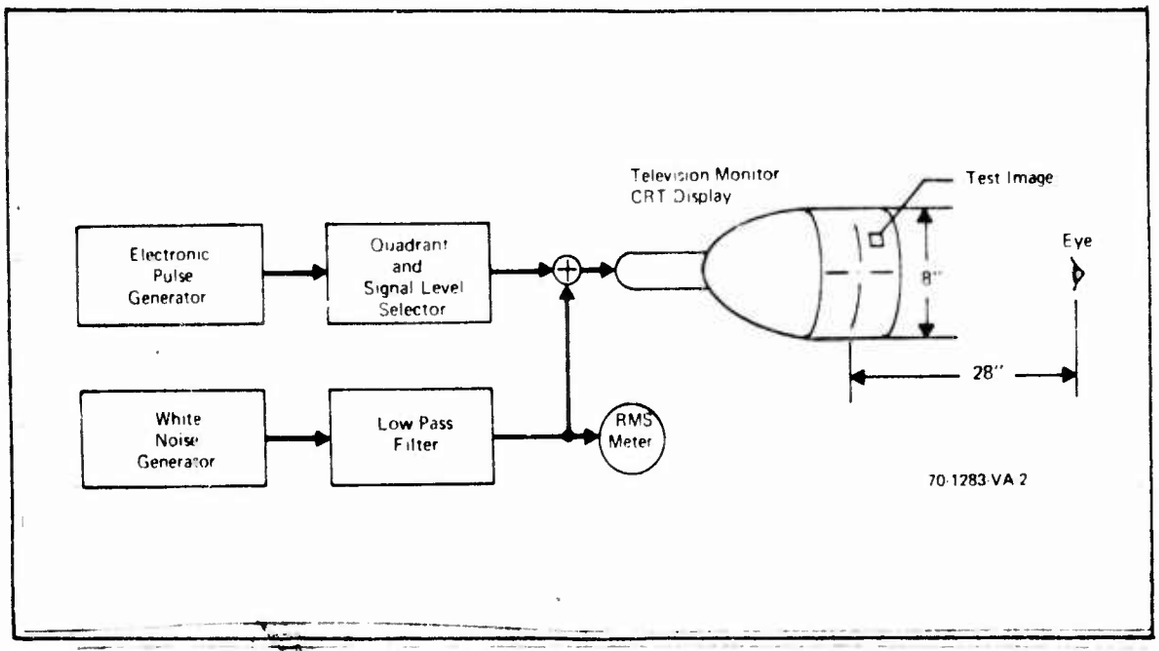

Figure 4 The Display Signal-to-Noise Ratio Experiment

noise ratios and image locations are randomly varied. The observer is asked to specify the image location whether he could see it or not. The probability of detection, determined in this manner was then corrected for chance using the formula

$$P_d = (P_o - P_c)/(1 - P_c) \quad , \tag{1}$$

where P_d is the corrected probability, P_o is the raw probability and P_c is the probability due to chance (0.25 for the case cited). Two noise bandwidths of 7.1 and 12.5 MHz were used and the observation time per trial was usually 10 seconds. The observer distance from the 8" high picture was 28" unless otherwise specified and the display background brightness was either 0.2 - 0.3 or 1 ft-Lambert. The television monitor was operated at 30 frames per second with a conventional 525-line scan in the vertical.

For convenience, we defined the image size in terms of

the dimension of a single scan line. Thus, the rectangle dimensions are

$$\Delta x \cdot \Delta y = (490)^2 \alpha\left(\frac{a}{A}\right) , \qquad (2)$$

where 490 is the number of active lines in a conventional 525-line television display and α is the width-to-height aspect ratio of the total effective picture on the CRT. The quantity a is the image area while A is the total picture area displayed. The video SNR is directly measurable. The video and the image SNR, though related, are not the same as we have discussed at length in Refs. (1-5). For the special case where the noise is white and where the image is large enough so that the sensor MTF's can be ignored, the displayed image SNR_D is

$$SNR_D = [2\Delta f_v t(\frac{a}{A})]^{\frac{1}{2}} SNR_V . \qquad (3)$$

where SNR_V is the video signal-to-noise ratio as measured in the video channel. Equation 3 is equation 77 in reference 2 and is a simplification of equation 163 in reference 5. We used the subscript D on SNR_D to differentiate it from SNR_p which is the SNR perceived by the observer. For displayed images that are bright enough and neither too large or too small, SNR_D will be very nearly equal to SNR_p.

In Fig. 5, we show the probability of detection corrected for chance as a function of the video SNR. The images ranged from a square 4 x 4 scan lines in size to a long rectangle subtending 4 x 180 lines. As can be seen, a large SNR_V is required to detect the small square while the long thin rectangles are readily detected with a very small SNR_V. By use of Fig. 5 and Eqs. (2) and (3), we can calculate SNR_D and plot the probability of detection as a function SNR_D as shown in Fig. 6. Observe that the four curves now plot as a single curve. The angular subtense of the rectangles

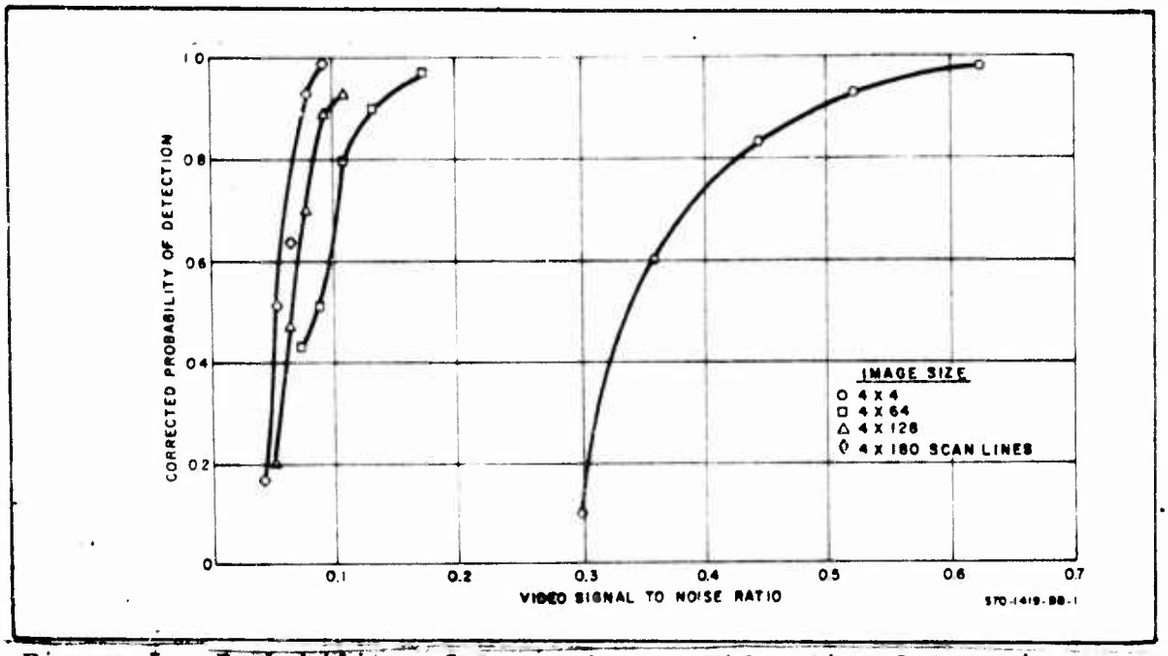

Figure 5. Probability of Detection vs Video Signal-to-Noise Ratio Required for Rectangular Images of Size ○ 4 x 4, □ 4 x 64, △ 4 x 128, and ◇ 4 x 180 Scan Lines. Televised Images at 30 Frames per Second. Observer-to-Display Viewing Distance/Display Height (D_V/D_H) = 3.5.

relative to the observer's eye varied from 0.13° x 0.13° to 0.13° x 6.2°. For these images, the eye acts as a near perfect spatial integrator. This is not true for images which subtend more than about 0.5° or 9 mr in both dimensions simultaneously. In Fig. 7, we show the result of an experiment using squares. Ignore the result for the 2 x 2-line square for the moment. The SNR_D needed to detect the 4 x 4 and 8 x 8-line squares is the same within the experimental error. However, a small increase is needed to detect the 16 x 16-line square which subtends 0.5° at the observer's eye and the increase has been found to be statistically significant. Substantial increases are needed to detect the 32 x 32 and 64 x 64-line squares. The reason is that the eye acts as a differentiator at edges. The long thin rectangles are nearly all edge, while the squares have substantial interior area.

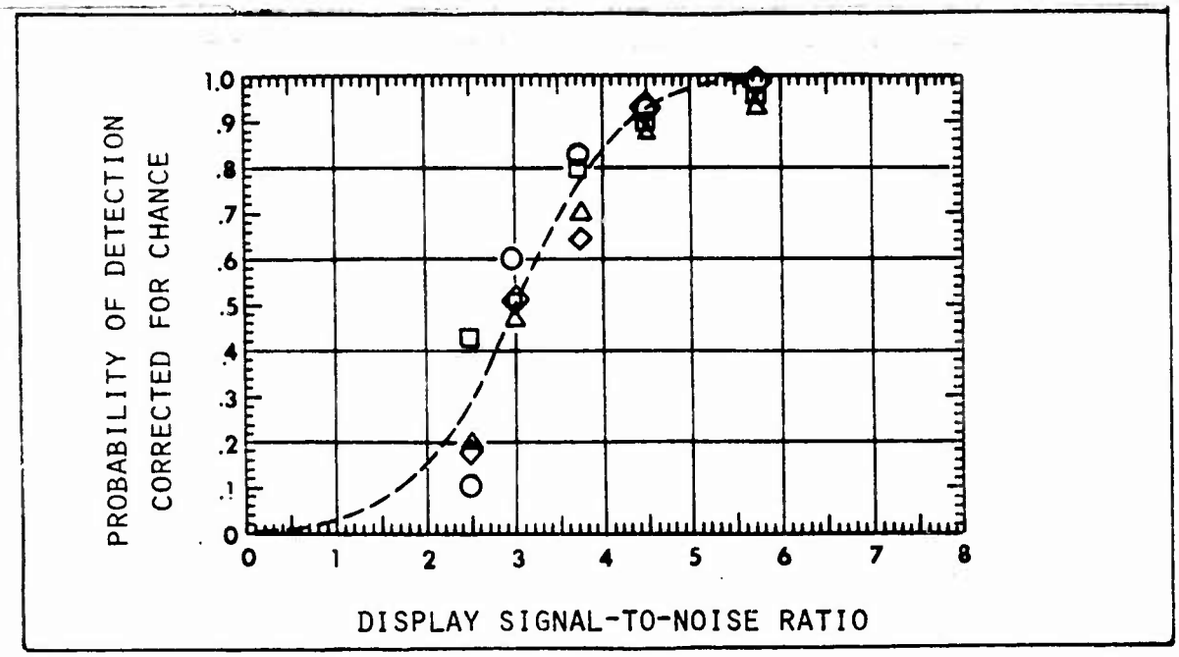

Figure 6 Corrected Probability of Detection vs SNR_D Required for Rectangular Images of Size ○ 4 x 4, □ 4 x 64, Δ 4 x 128, and ◇ 4 x 180 Scan Lines. Televised Images at 30 Frames per Second and 525 Scan Lines. D_V/D_H = 3.5.

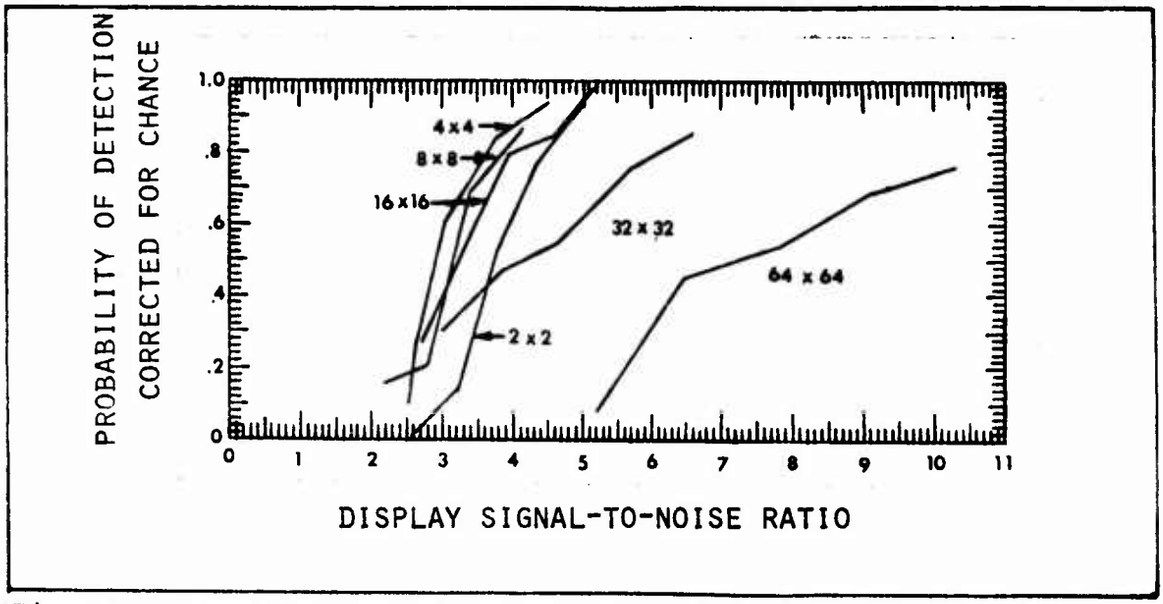

Figure 7 Probability of Detection vs SNR_D for Squares of Various Size at a Display Distance to Height Ratio of 3.5.

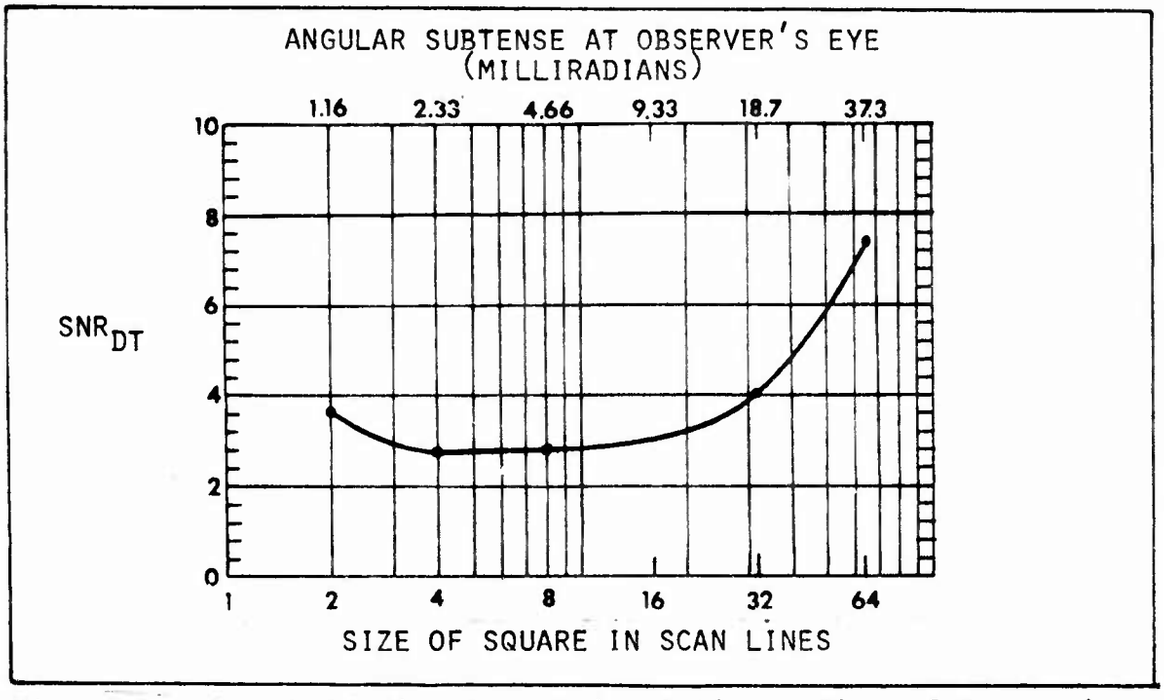

Figure 8 Threshold Signal-to-Noise Ratio vs Size of Square in Scan Lines. D_V/D_H = 3.5.

The threshold SNR_D's, corresponding to a 50% probability of detection are plotted in Fig. 8. Note the increase in SNR_D needed for the 2 x 2-line square. This square subtends about 1 mr at the eye. The noise equivalent aperture, δ_e, of the eye is believed to be about 1 mr (δ_e is the reciprocal of the noise equivalent bandpass N_e). If this is so, we would expect a small increase in threshold SNR_D or SNR_{DT}. Stated differently, the ability of the observer to detect images of size smaller than about 1 mr will be limited by the MTF of the observer's eye. The threshold SNR_{DT} required for various square sizes are summarized below in Table 1 for the various squares at a viewing distance to display height D_V/D_H ratio of 3.5. If the viewing distance is doubled using the same display, the SNR_{DT} applying to a 4 x 4-line square becomes that for a 2 x 2 square as illustrated in the Table 1.

TABLE 1 THRESHOLD SNR_{DT} vs SQUARE SIZE FOR TWO DISPLAY DISTANCE TO DISPLAY HEIGHT RATIOS

Image Size (Scan Lines)	SNR_{DT} $D_V/D_H = 3.5$	SNR_{DT} $D_V/D_H = 7.0$
2 x 2	3.7	-
4 x 4	2.8	3.7
8 x 8	2.8	2.8
16 x 16	3.3	2.8
32 x 32	4.0	3.3
64 x 64	7.5	4.0

As has been discussed, the primary effect of display viewing distance to height ratio is to change observer thresholds somewhat when the observer is comfortably viewing a stationary display. The change is not large for square images which subtend angles from 1 to 15 mr at the observer's eye. In a severe vibration environment, one would expect the detectability of small images to be degraded more than that of larger images and thus it would appear desirable to emphasize the smaller images in the experimentation.

The current square (and rectangular) image generator has a capability of generating squares of size 2 x 2 to nearly full screen in size. A 1 x 1 is not possible due to the interlace of the display and the method of generating pulses. Thus to make images smaller relative to the observer's eye, it becomes necessary to either increase observer viewing distance or use a smaller display.

It was originally planned to employ a display viewing distance-to-height ratio of 3.5 as was used in the majority of the previous lab tests. For a monitor of 9" diagonal

and 5.4" height, the viewing distance would be 18.9" and the smallest 2 x 2-line image would subtend 1.2 mr. To emphasize small images, we would like to decrease image angular subtense to 0.5 to 0.6 mr which would employ an increase of viewing distance to 38" for the 9" diagonal monitor. However, as can be seen from Fig. 9, display viewing distances more than 28" were not possible. In Fig. 10, we show the angular subtense of the 2 x 2 square as a function of viewing distance for various display diagonals. It is seen that a 0.78 mr angular subtense is obtainable with the Panasonic 9" display at the 28" viewing distance.

3.2 Experimental Procedure

The squares are of size 2 x 2, 4 x 4, 8 x 8, and 16 x 16 scan lines. In the ground tests, about 5 SNR values, appropriately selected were sufficient to define the probability of detection vs SNR_D curve for each square. However, more SNR_D values were needed in the flight test to allow for the expected degradation - at least for the smaller squares. Therefore, 8 values of SNR_D were used for the 2 x 2 square, 7 for the 4 x 4 square, and 5 each for the other two sizes. Ideally, there would be 100 data points per observer per experiment.

It was originally planned to generate the test images with the electronic pulse generator, video tape the images at various SNR_D levels and use the taped images for the psychophysical experiments in both the ground based and in flight tests. While this represents considerable convenience in performing the experiments, the recorder MTF severely limits spatial frequency response and may have vibration problems. Upon further investigation it was found to be possible to use the electronic image generator which is a technically superior approach.

The SNR_D, square size and square position are all randomly selected. The procedure is to construct a table of the total

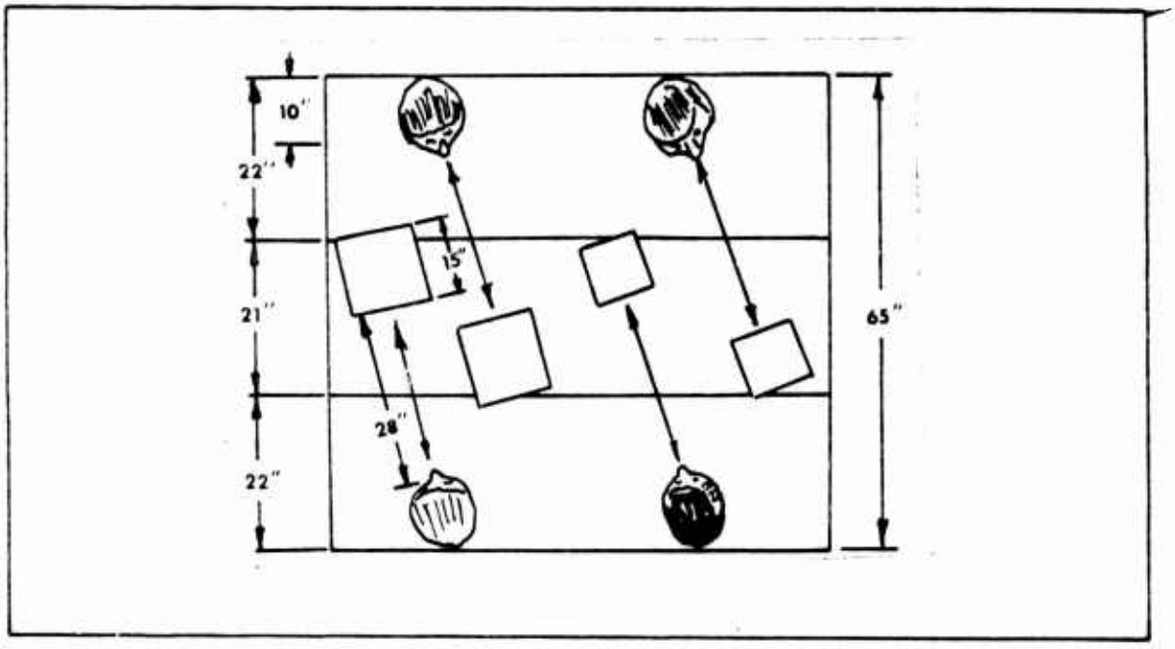

Figure 9 Layout of Observer's Compartment

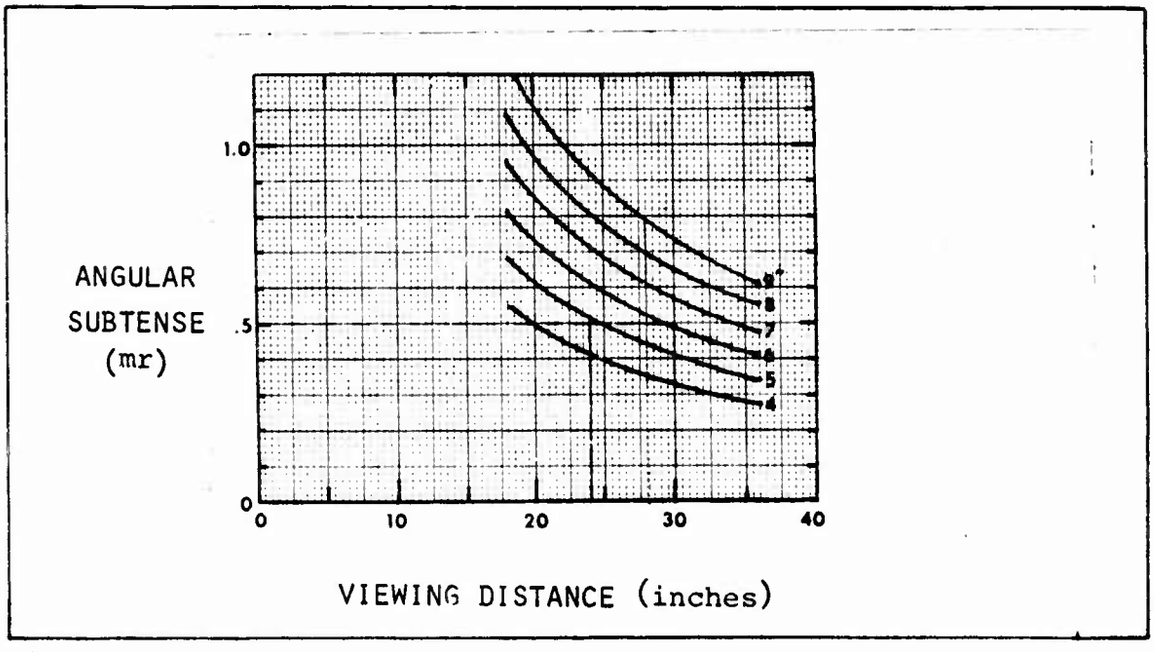

Figure 10 Angular Subtense of 2 x 2 Square at the Observer's Eye as a Function of Viewing Distance for Various Display Diagonal Dimensions.

experiment as shown in Table 2. The order in which each experiment is performed is selected on the basis of a random number table and a new table is set up in numerical order as shown in Table 3 representing the type of test controller sheet which was used. The particular SNR_D values were selected on the basis of a preliminary experiment to determine the range needed. The observer records on a pad the quadrant he thinks the square is in for each observation during the time period between individual tests while the controller is setting up for the next test. A typical test data sheet is shown in Table 4.

Prior to every flight, the test operator performed the checklist operations below as referenced in Table 5.

1. Data Forms, Pens

Determine that the total number of data forms needed for the experiments and that an adequate supply of felt pens is available. The data forms include those for the observer and the experiment operator.

2. Equipment Warm-up

Turn on all electronic equipment and check voltage levels. Allow the equipment to stabilize prior to final setup.

3. Check Equipment Hookup

Determine that all equipment is hooked up and that line terminations are on correctly.

4. Preliminary Equipment Test

Approximately adjust TV monitors. Apply noise from noise generator. Check that position/size switches are working properly.

5. Equipment Calibration and Set-up

After warm-up period, calibrate and perform final equipment set-up.

TABLE 2 RECTANGULAR IMAGE TEST

QUADRANT	IMAGE SIZE			
	2 x 2	4 x 4	8 x 8	16 x 16
1	S/N - 1 S/N - 2 S/N - 3 S/N - 4 S/N - 5 S/N - 6 S/N - 7 S/N - 8	S/N - 1 S/N - 2 S/N - 3 S/N - 4 S/N - 5 S/N - 6 S/N - 7	S/N - 1 S/N - 2 S/N - 3 S/N - 4 S/N - 5	S/N - 1 S/N - 2 S/N - 3 S/N - 4 S/N - 5
2				
3				
4				

TABLE 3 TYPICAL TEST CONTROL SHEET

CONTROLLER SHEET - RECTANGULAR IMAGE TEST (RUN TWICE)

NAME _____ DATE _____ TIME _____

SIGNAL (0 db) = _____ FLIGHT PATTERN _____

NOISE (0 db) = _____ WEATHER _____

#	T	db	Q	TIME M	TIME S	COMMENTS	#	T	db	Q	TIME M	TIME S	COMMENTS
1	4x4	8	3				26	4x4	8	4			
2	16x16	21	4				27	2x2	9	2			
3	4x4	18	2				28	16x16	25	2			
4	2x2	0	3				29	2x2	3	4			
5	4x4	20	4				30	4x4	10	2			
6	8x8	19	4				31	4x4	16	4			
7	2x2	10	3				32	16x16	21	1			
8	16x16	25	1				33	8x8	25	4			
9	4x4	10	3				34	4x4	14	3			
10	8x8	17	2				35	16x16	29	1			
11	2x2	6	4				36	2x2	7	3			
12	4x4	8	2				37	8x8	19	3			
13	8x8	23	1				38	4x4	18	4			
14	4x4	18	3				39	2x2	1	4			
15	2x2	4	2				40	4x4	16	3			
16	16x16	27	3				41	8x8	21	3			
17	4x4	20	2				42	2x2	0	1			
18	16x16	27	4				43	8x8	25	2			
19	4x4	16	2				44	2x2	6	1			
20	8x8	25	1				45	4x4	14	2			
21	2x2	9	4				46	16x16	29	2			
22	4x4	12	2				47	4x4	18	1			
23	16x16	23	3				48	2x2	4	1			
24	8x8	23	2				49	16x16	25	3			
25	16x16	27	1				50	4x4	8	1			

TABLE 4 TYPICAL OBSERVER TEST SHEET

OBSERVER SHEET - RECTANGULAR IMAGE TEST

MONITOR # _____

NAME _____ DATE _____ RASTER SIZE _____

#	QUADRANT 1	2	3	4	COMMENTS	#	QUADRANT 1	2	3	4	COMMENTS
1						26					
2						27					
3						28					
4						29					
5						30					
6						31					
7						32					
8						33					
9						34					
10						35					
11						36					
12						37					
13						38					
14						39					
15						40					
16						41					
17						42					
18						43					
19						44					
20						45					
21						46					
22						47					
23						48					
24						49					
25						50					

GENERAL COMMENTS:

TABLE 5 PREFLIGHT CHECKLIST

Observer Data Forms Available	____
Experimenters Data Forms Available	____
Pens Available	____
Equipment Warm-up, Turn On	
Noise Generator	____
Monitors (4)	____
Image Generator	____
AR-200 Recorder (Warm-up)	____
CRT Oscilloscope	____
Charge Amplifiers	____
Check Equipment Hook-up	
Image Generator	____
Square Size Selector	____
SNR_D Selector	____
Noise Generator	____
TV Monitors (4)	____
AR-200 Recorder	____
Charge Amplifiers/Accelerometers	____
Preliminary Equipment Test	
Approximate TV Monitor Adjust	____
Add Noise	____
Check Square Position Selector	____
Check Square Size Selector	____
Equipment Calibration and Set-Up	
Adjust Noise & Signal Levels	____
Monitor Brightness & Contrast	____
Recheck Size & Position of Squares	____
Check Accelerometers	____

6. Calibrate Noise Generator

Measure rms noise using rms meter.

7. Adjust Display Brightness

Set the TV monitors to the preselected brightness levels of 2 f-L using a calibrated meter.

8. Adjust Display Contrast (Gain)

Adjust video gain (contrast) of each monitor to the appropriate level by applying maximum signal and noise so that the brightness level increased to 4 f-L.

9. Signal Levels

Use oscilloscope to determine that all signal levels are correct.

10. Recheck Operation of Position Size Switches

Check to see that square size and position can be varied by observation on display.

11. Acceleration Measurement Equipment

Check out and calibrate the 3-axis accelerometers, charge amplifiers, and 14-channel tape recorder used to monitor the acceleration in the aircraft.

Once the aircraft had landed, the equipment was rechecked to ascertain that there were no departures form the initial nominal values. Only in flight no. 3 were departures measured. In flight, the observers had the window blinds down and a black cloth separated the baggage compartment where the experimenter was located from the passenger compartment. The approximate ambient light level during the experiment was less than 1 f-L. No contrast loss on the monitors could be measured due to the ambient.

3.3 Analysis of Data

Four flights were flown during the first half of the program and a total of 1,928 data points were taken for all conditions. In Table 6, a summary of the data points and conditions for the four flights is shown for the four observers.

TABLE 6 THE NUMBER OF DATA POINTS TAKEN EACH FLIGHT FOR VARIOUS CONDITIONS FOR SQUARES

Flight No.	Condition			
	Straight & Level	Rough Air	2½ g Turns	1½ g Turns
1	400	40	32	20
2	324	28	48	
3	60	400	56	
4	60	400	60	

The first flight was primarily dedicated to determining if there were any errors in our setup which would make it difficult to run the experiments in the air. One complete run was made under straight and level conditions; then 8 data points (32 for the four observers) were taken during 2½ g turns; 5 data points were taken during 1½ g turns; and 10 data points were taken under rough air conditions of about $\pm$ 0.2 g "bumps."

An analysis of the data indicates that a) no effect due to 1½ g turns could be seen, b) only a slight (if any) effect due to 2½ g turns could be seen, c) rough air did affect the data, and d) straight and level data was virtually identical to the lab data. The experimenter reported feeling ill during the 2½ g turns and he experienced great difficulty

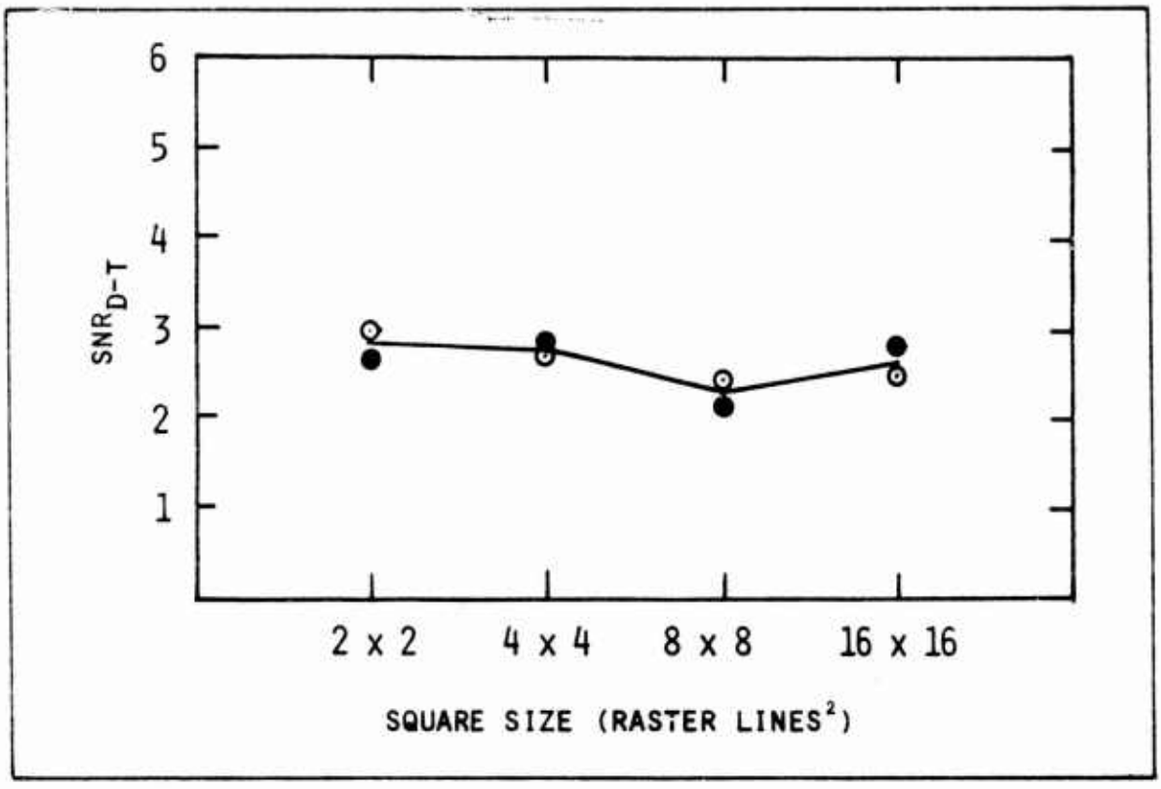

Figure 11 Threshold SNR_{DT} as a Function of Square Size for (o) Straight and Level Flight and (●) Lab Conditions.

working the rotary dial attenuator so before the next flight it was replaced by a rocker arm attenuator which was positioned very close to his seat. The experimenter's difficulties with resisting motion effects were due to his seating position and the need for operating the equipment during flight. This position, which was transverse to the aircraft axis, prevented him from bracing his abdominal muscles during g maneuvers.

In Fig. 11, the threshold SNR_D are shown for the straight and level conditions in flight. The lab data is also shown for the same observers. The data for both conditions are within 10% of the classic values discussed in section 3.2.

The plan for flight no. 2 was to gather data under 2½ g turns but after 8 data points the operator was sick and one of the observers was not feeling well either so the 2½ g turn portion of the flight was terminated. Then 8 points per man

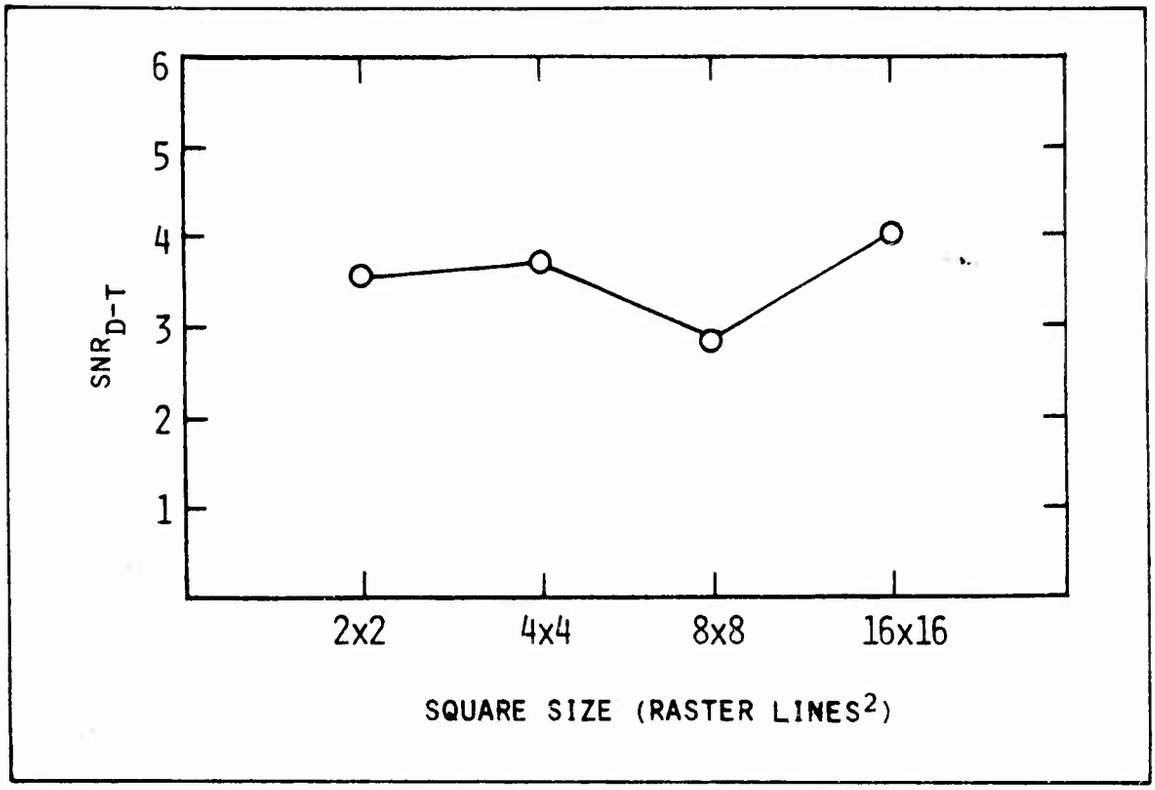

Figure 12 Threshold SNR_{D-T} as a Function of Square Size for Straight and Level Flight after 2½ g turns and ± 0.4 g Turbulence, Flight No. 2.

of rough air data, ± 0.4 g bumps were taken. Straight and level data was then taken (81 points per man). No problems were encountered during either the rough air portion of the flight or the straight and level portion.

In Fig. 12, the data for the straight and level portion of flight no. 2 is shown. Notice that, in general, the SNR_{D-T} values for flight no. 2 are higher than those for flight no. 1. Based on the very close correspondence between the lab data and the first straight and level data, it seems likely that either the signal levels were slightly higher, or the noise levels were slightly less (or both) for flight no. 2. Data taken in the last portion of the flight test program with bar patterns

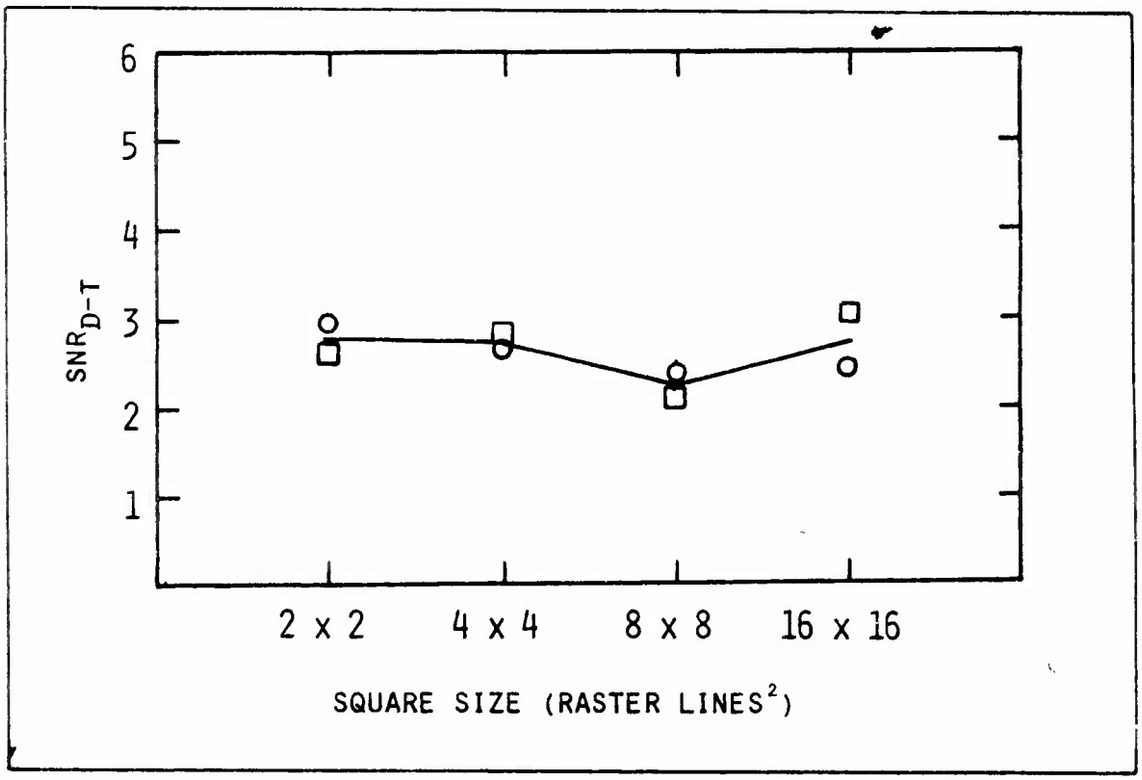

Figure 13 Threshold SNR_{D-T} as a Function of Square Size for Straight and Level Flight for Two Flights. o Flight #1 Data and □ Rescaled Data From Flight #2.

clearly shows that flying either turbulence or steady g loads first and then flying straight and level does not affect straight and level thresholds so their influences are unlikely to have been factors here.

If the straight and level data from flight no. 2 are adjusted so that the average value, for the four squares, is the same as that from flight no. 1, it is seen that the form of the data is the same in the two cases. The adjusted straight and level data from flight no. 2 and the straight and level data from flight no. 1 are plotted in Fig. 13.

The goal of flight no. 3 was to gather an adequate amount of data under turbulent conditions and this was accomplished; 100 data points were gathered per man. The turbulence was

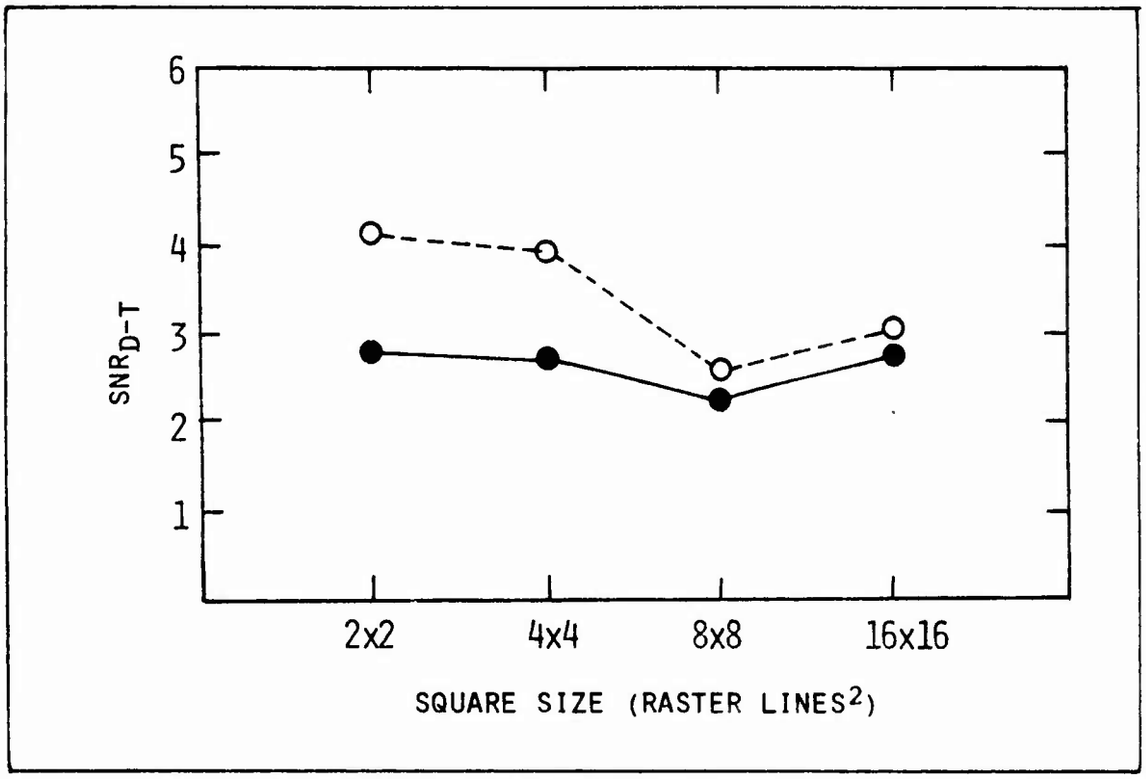

Figure 14 Threshold SNR_{D-T} as a Function of Square Size for ± 0.2 g, 1 sec Period Turbulence, o Flight No. 3 Data and ● Average Straight and Level Data.

approximately ± 0.2 g at about a 1 sec interval, but varied from ± 0.2 g to ± 0.6 g at times. Two sets of 7 data points per man each at 2½ g were also taken interspersed with an equal amount of straight and level data to prevent operator upset. The technique was successful.

In Fig. 14, the data for the turbulence conditions is plotted. The turbulence definitely affected the threshold for both the 2 x 2 and the 4 x 4 size squares but apparently had little effect on the larger squares. Approximately 33% more SNR_D is required for the smallest squares. A post flight check showed that the noise was less than was thought and a subsequent checkout of the noise generator indicated a replacement of the noise tube was called for. A comparison of the data for the first half of the flight with that for the

last half showed that the data was virtually the same and whatever the noise level really was, it was reasonably constant during the whole flight.

Taking more data under turbulent conditions was the goal of the fourth flight and this was accomplished. Two sets of 2½ g data were also taken, interspersed with an equal amount of straight and level data. The turbulence was $\pm$ 0.2 to $\pm$ 0.5 g with occasional peaks to 0.8 g but at about one-half the frequency of the previous flight; about 3 sec per cycle at first part of the flight and about 1 sec per cycle at the end. The data from the turbulent portion of the flight is plotted in Fig. 15. Again, the data suggests a higher threshold for the small squares than the other squares but the whole scale appears to have been shifted as the threshold for the larger two squares is 23% lower than was found in flight no. 3.

The data from flight no. 3 for turbulence shows that the threshold for the large squares (8 x 8 and 16 x 16) is only 14% higher than that obtained under straight and level conditions. Thus we can have reasonable confidence that turbulence of the type encountered has little effect on larger squares. A comparison of the largest square data between the two turbulent conditions of flight nos. 3 and 4 shows that the last set of data is 35% lower. Assuming that an error in noise measurement was made, we will shift the scale on all of the data for flight no. 4 by a factor of 1.31 which of course gives the same average SNR_D for the large square for the two experiments under turbulent conditions. Doing this and replotting the data in Fig. 15 shows there is a definite effect due to turbulence on flight no. 4 also, and the two sets of data are similar.

In Fig. 16, the data from the four flights and the lab test are plotted. Straight and level data from flight no. 1 have been averaged with the lab data and is represented by the solid line in the figure. The data from the two turbulent conditions

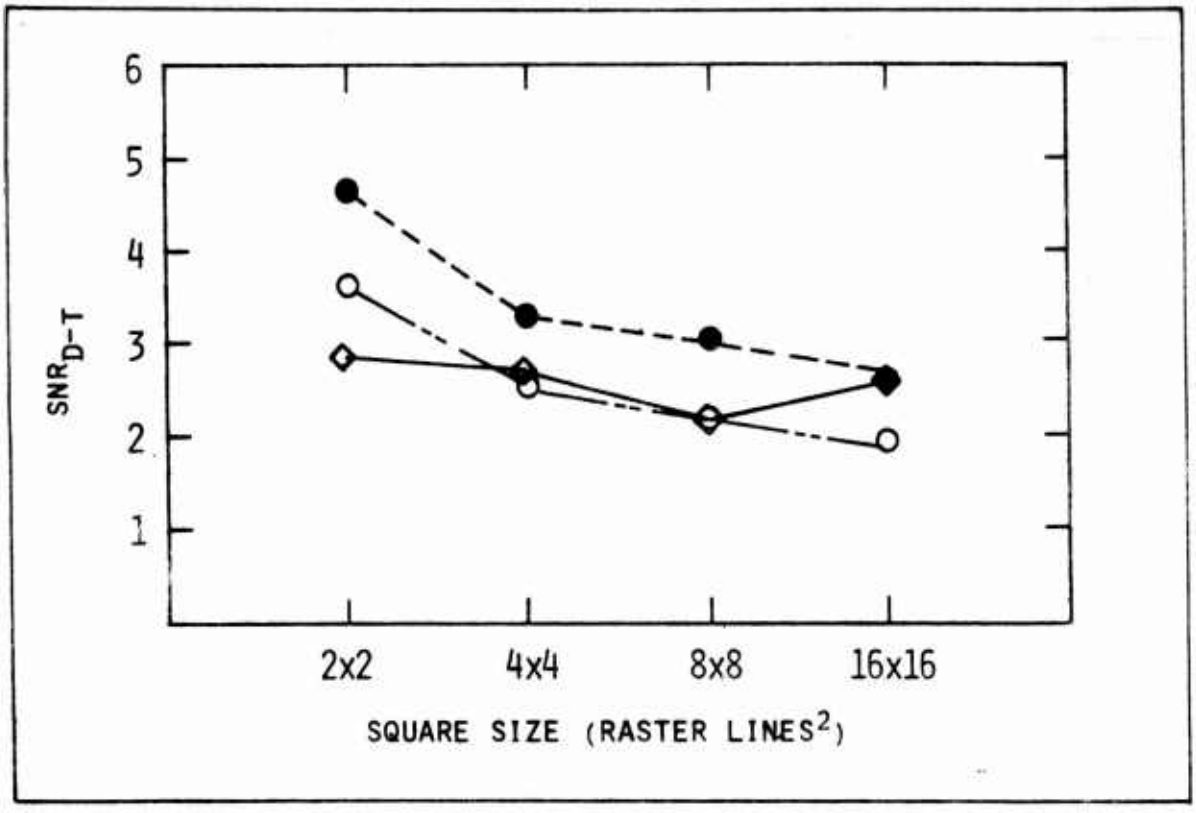

Figure 15 Threshold SNR_{D-T} as a Function of Square Size for ± 0.35 g, 2 sec Period Turbulence. o Flight No. 4 Data, ◇ Average Straight and Level Flight and ● Rescaled Data for Turbulent Conditions.

have also been averaged and this is represented by the dashed line.

The ratio of the solid curve (average between lab data and straight and level for flight no. 1) and the dashed curve (average data under turbulence) is plotted in Fig. 17 and represents the size effect, due to the average turbulence for the experiment. Notice the reversal in the scale for size for convenience of the plot.

It is interesting to note that, for the average turbulence conditions represented by the experiment, an exponential relationship is suggested by the data of Fig. 17

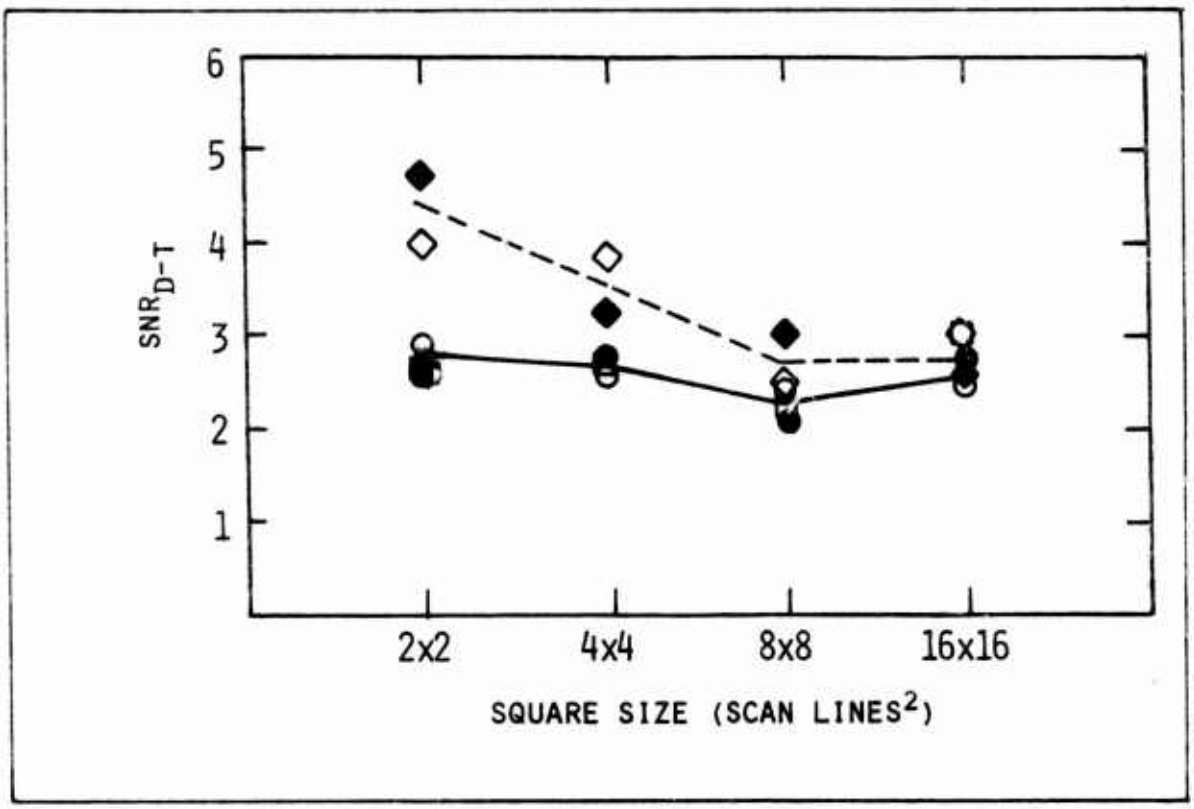

Figure 16 Threshold SNR_{D-T} as a Function of Square Size for the Four Flights and Lab Comparison Data; ● Lab, o Straight and Level Flight No. 1, □ Straight and Level Flight No. 2 (Scaled), ◇ Turbulent Flight No. 3, ◆ Turbulent Flight No. 4 (Scaled).

for the relationship between the ratio and square size. This is analogous to the effects due to random motion of the input photocathode of an electro-optical integrating sensor.

An analysis of all of the g data shows very little, if any, effect due to the g loading. An inadequate amount of g data was taken during the first four flights and a major goal of the next flights was to get adequate g data. As will be seen, this goal was met.

For these four flights, all of the accelerometer data was obtained from the accelerometer in the cockpit. Instrumentation difficulties prevented collecting useful data from the observer compartment.

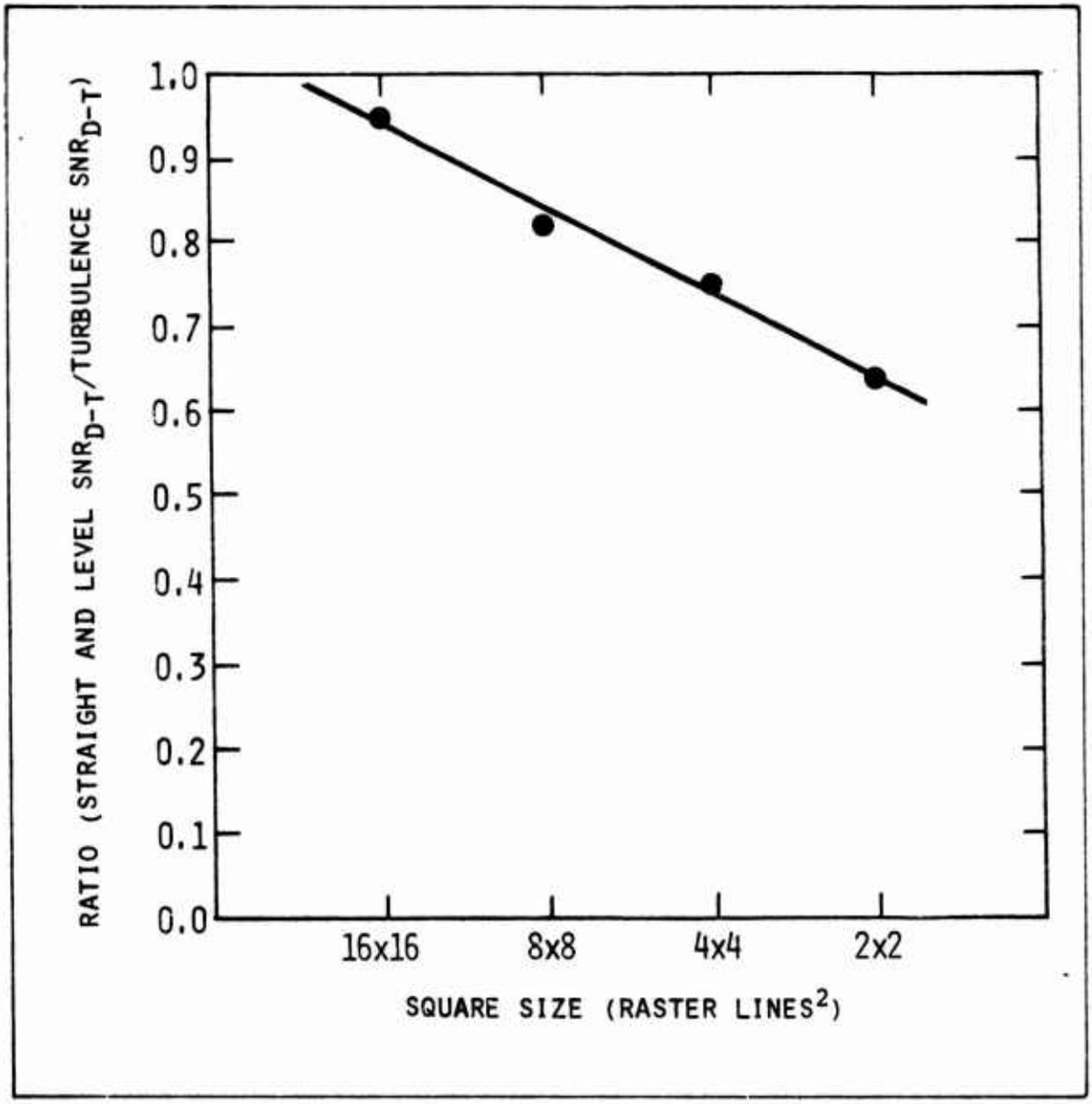

Figure 17 Ratio Between Threshold SNR_{D-T} for Squares for Average of Straight and Level, and Lab Data to the Average Data for Turbulent Conditions.

3.4 Operator Comments

A brief form was generated to gather operator comments on the flight test. For the first four flights, six different observers flew, two of which have had extensive experience in high performance aircraft.

Once the observers were familiar with liminal perception of squares, little individual difference in threshold was noted. Observers with high performance aircraft experience usually experienced less discomfort during 2½ g turns or during turbulence.

The observers' opinions were that 2½ g turns did not hinder their ability to detect. There was speculation that pulling into and pulling out of the turns would effect their threshold much more.

Those who had F-4 experience thought that the flight response of the Saberliner was similar to the F-4 under most conditions. In smooth air the flight characteristics and sensations are almost identical. The g loading fell quite short from the 6+ g's experienced in F-4's. The short turn medium amplitude turbulence was almost identical to the sensations experienced flying F-4's through choppy air.

In general, the observers thought that turbulence made it more difficult to detect the squares due to the search problem (much more work was required to search out the four quadrants). As will be seen in the next section, turbulence (of a smaller amount) had less effect on bar pattern recognition than it did on square detection.

The observers thought that they fatigued after taking 60 data points or so but the data does not show this fatigue. A specific example of this will be shown in the next section on bar pattern resolution.

4.0 EXPERIMENTS USING PERIODIC IMAGES

The ability of an observer to discern bar patterns on the display of an imaging sensor is often used as a measure of the ability of the sensor to resolve scene detail. Psychophysical experiments using bar patterns are somewhat more difficult to construct and interpret than are the aperiodic objects such as rectangles. The bar pattern experiments cannot be easily randomized in location as were the squares and the results are somewhat subject to operator training and experience. It is, of course, much easier to detect squares and rectangles than to discern individual bars in a bar pattern and thus the ability to resolve bar patterns is a more sensitive test of system capability.

4.1 Review of Previous Work

The basic experimental apparatus employed is shown schematically in Fig. 18. Bar patterns of various height-to-width ratios, spatial frequencies and numbers of bars in the pattern were constructed and were projected on the faceplate of a high resolution 1½" vidicon operated at highlight video signal-to-noise ratios of 50:1 or better. The camera and TV monitor were operated at 25 frames per second and 875 scanning lines. Band-limited while noise of Guassian distribution was mixed with the camera generated signal. Both the signals and noises were passed through identical 12.5 MHz filters prior to mixing in the monitor. The monitor luminance was approximately 1 ft-Lambert unless otherwise stated.

In the psychophysical experiments, the test images were bar patterns of various kinds and the observer was required to

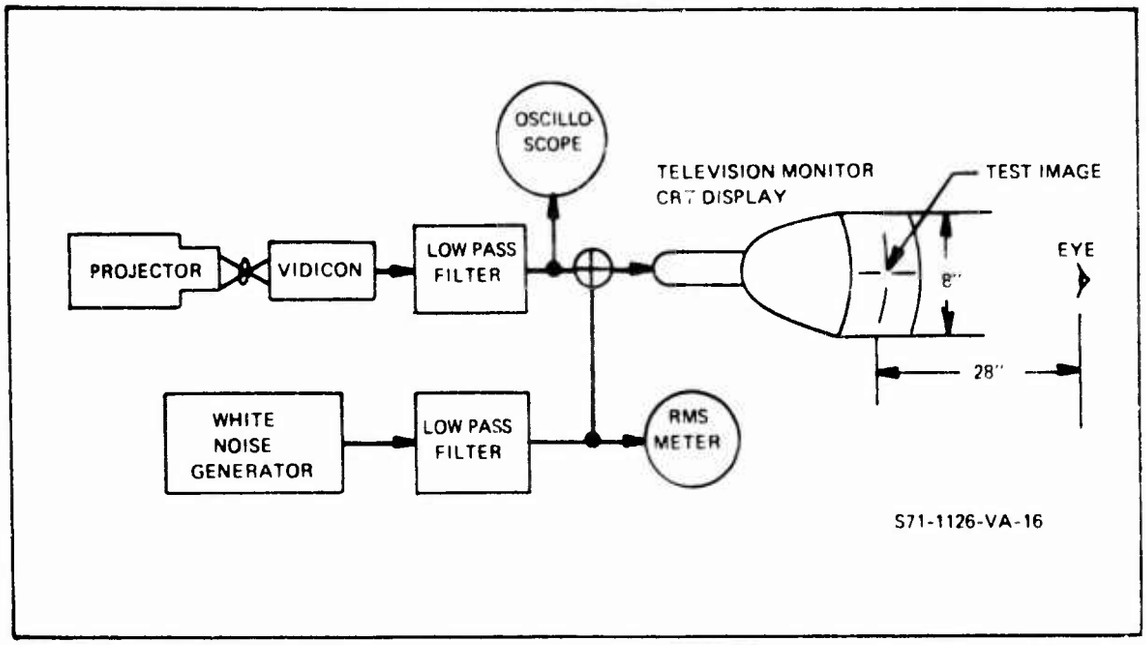

Figure 18 Experimental Setup for Television Camera Generated Imagery.

state whether or not the pattern displayed was resolvable as the image SNR's are randomly varied. Chance is not involved since the patterns were always present on the display. A typical result is shown in Fig. 19 where the effort was to determine the effect of bar length-to-width ratio. For the 396-line pattern, little effect of bar length to width ratio is noted (it is assumed that the observer spatially integrates over the full length of the bar in making the SNR_D calculation). At lower spatial frequencies, this is not true as can be seen by the threshold SNR_D variation in Fig. 20. In Fig. 21, the SNR_D required to detect bar patterns was determined as a function of spatial frequency holding bar length-to-width ratio equal to 5. In the above experiments, the SNR_D's were randomly varied. In Fig. 22, we compared the thresholds obtained by varying SNR_D randomly with that obtained using "the method of limits." In the "method of limits," a number of bar patterns, each with a progressively higher spatial frequency

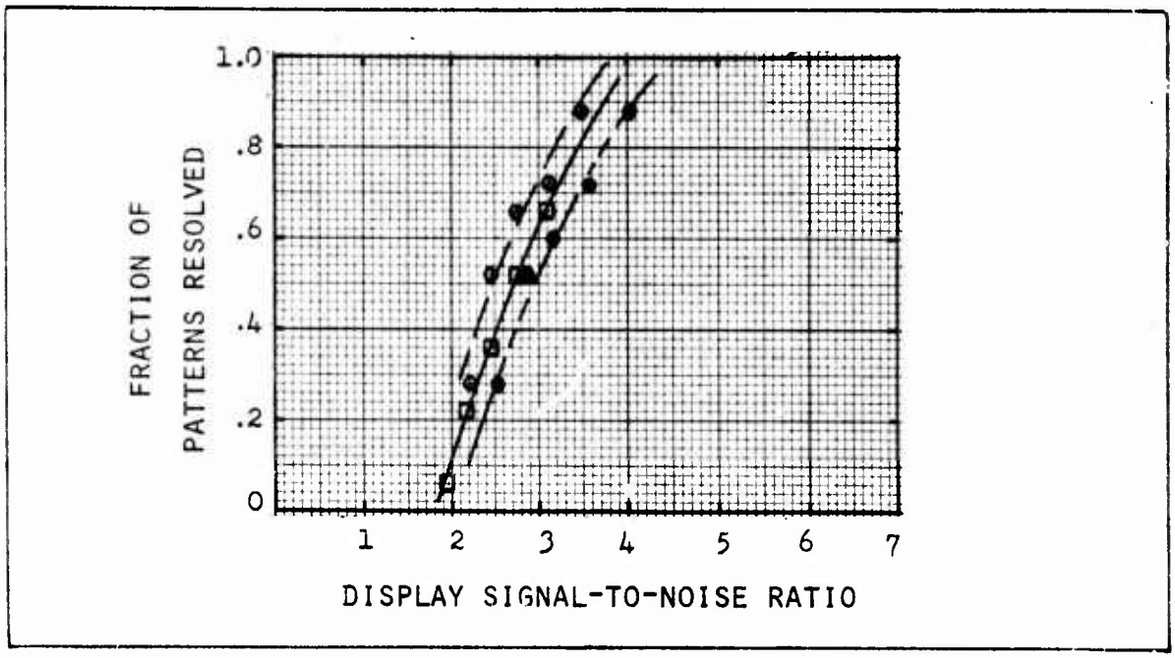

Figure 19 Fraction of Bar Patterns Resolved vs Display Signal-to-Noise Ratio for a 396-Line Bar Pattern of Length-to-Width Ratio □ 5:1, O 10:1, ● 20:1 Televised Images at 25 Frames/Sec. 875 Scan Lines, D_V/D_H = 3.5.

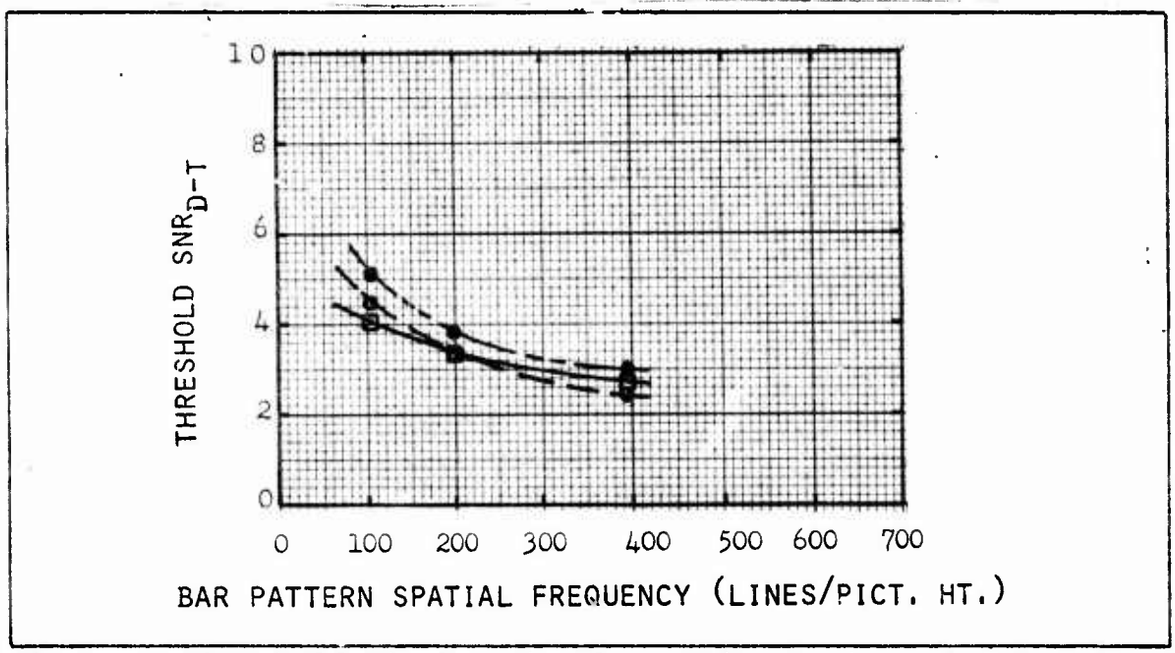

Figure 20 Threshold Display Signal-to-Noise Ratio vs Bar Pattern Spatial Frequency for Three Bar Length-to-Width Ratios of □ 5:1, O 10:1, ● 20:1 Televised Images at 25 Frames/Sec. 875 Scan Lines, D_V/D_H = 3.5.

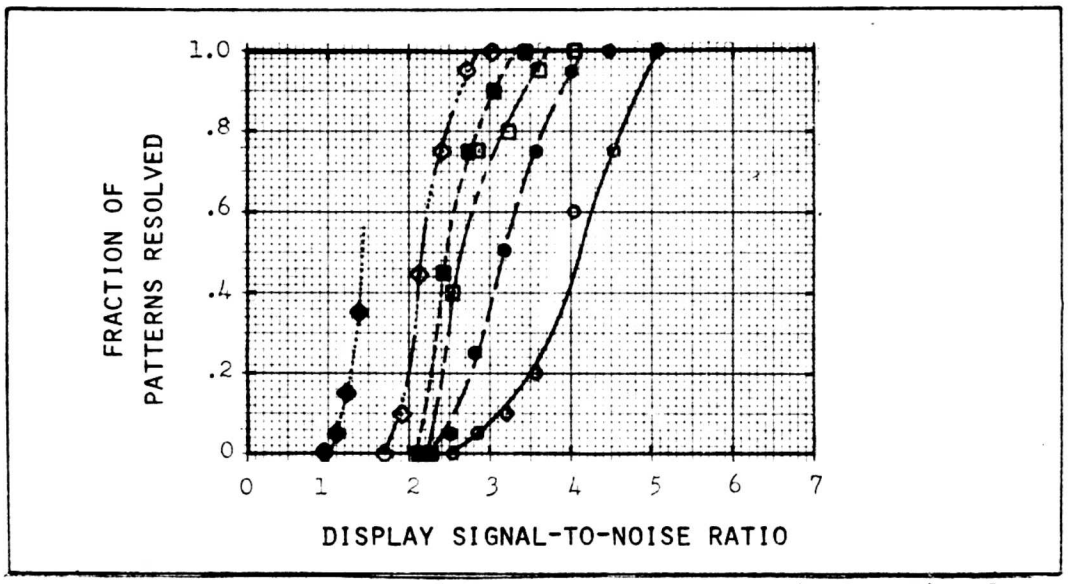

Figure 21 Fraction of Bar Patterns Resolved vs Display Signal-to-Noise Ratio for Bar Patterns of Spatial Frequency ○ 104, ● 200, □ 329, ■ 396, ◇ 482 and ◆ 635 Lines per Picture Height. Bar Height-to-Width Ratio was 5 in All Cases. Televised Images at 25 Frames/Sec. 875 Scan Lines, $D_V/D_H = 3.5$.

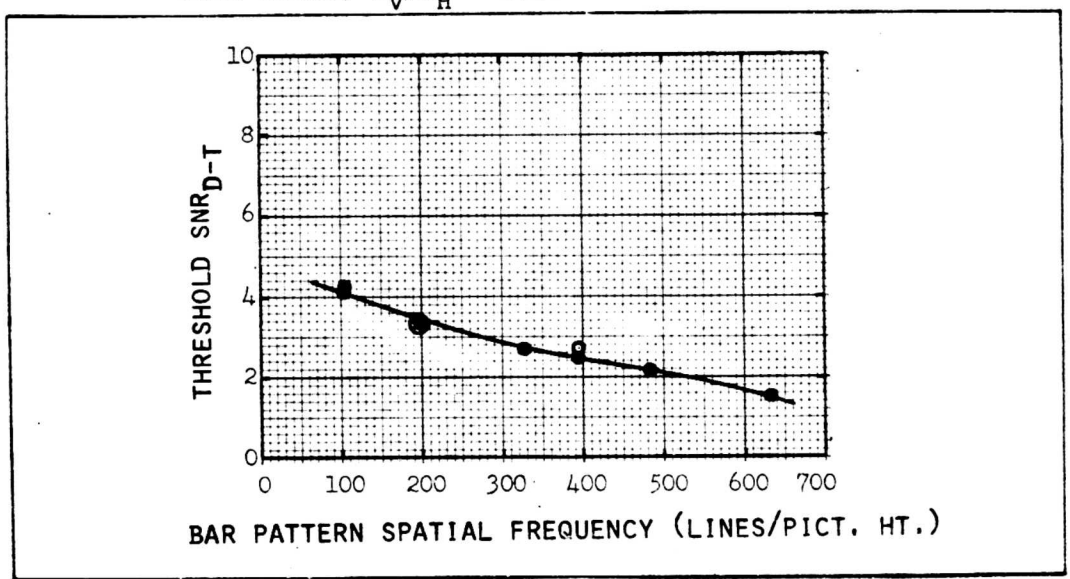

Figure 22 Threshold Display Signal-to-Noise Ratio vs Bar Pattern Spatial Frequency Obtained Using Two Different Experimental Techniques; ● Method of Limits and ○ Method of Random SNR Variation. Televised Images at 25 Frames/Sec. 875 Scan Lines, $D_V/D_H = 3.5$.

were simultaneously displayed and the observer was asked to select the pattern of highest frequency which he could just barely discern as the signal-to-noise ratio was varied (usually in a cyclical manner up and down). The two methods give essentially identical results.

In Fig. 23, we show the effect of display viewing distance to display height ratio, D_V/D_H (1.75:1, 3:5:1 and 7:1) on the detection threshold. It is clear from the figure that an increase in distance aids the detection of low frequency patterns at the expense of the high frequency patterns and conversely a decrease in distance aids the detection of high frequency patterns at the expense of the low frequency patterns.

The display signal-to-noise ratio is calculated using the formula

$$SNR_D = \left[\frac{2t\varepsilon\Delta f_v}{\alpha}\right]^{\frac{1}{2}} \frac{R_{sf}(N)}{N} \left(\frac{\Delta V}{V_n}\right) , \qquad (4)$$

where $\Delta V/V_n$ is the peak-to-peak signal to RMS noise ratio, ε is

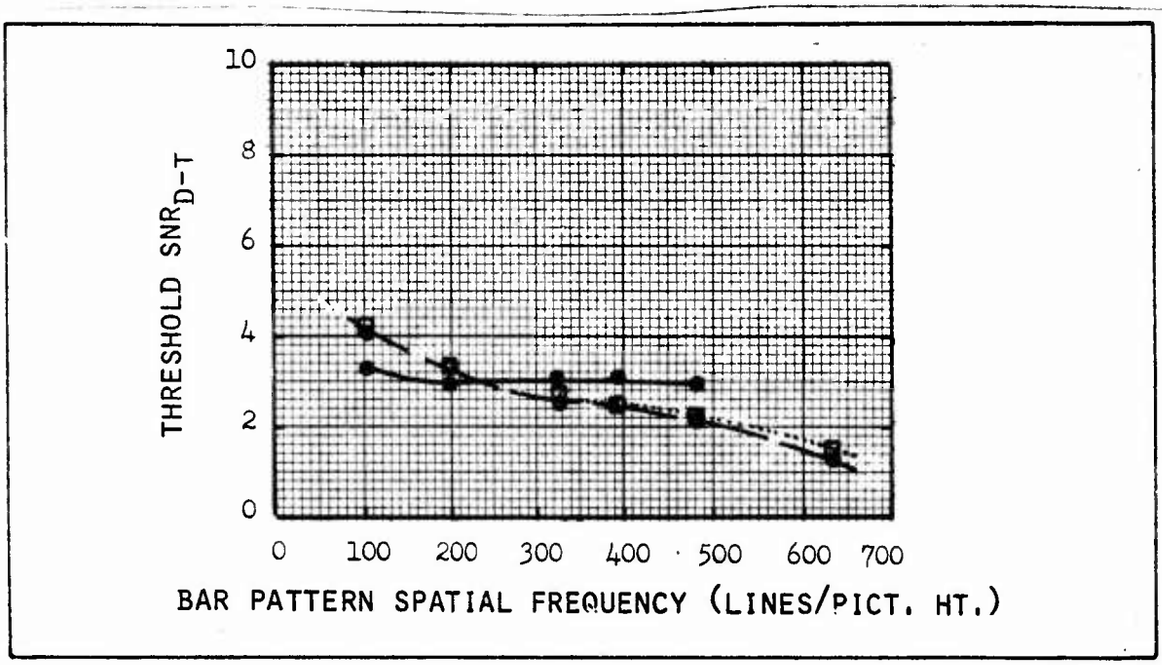

Figure 23 Threshold Display Signal-to-Noise Ratio vs Bar Pattern Spatial Frequency for Display to Observer Viewing Distances of O 14", □ 28", and ● 56". Televised Images at 25 Frames/Sec and 875 Scan Lines.

the bar height-to-width ratio, N is the bar pattern spatial frequency in lines/picture height and $R_{sf}(N)$ is the square wave flux response of the image generator if different than one.

4.2 Experimental Procedure

Again, the original notion was to video tape the various bar patterns for in-flight presentation. Apart from the possible tape recorder vibration problem, the most serious problem is that of tape recorder bandwidth. With the type of recorder originally planned, the highest spatial frequency which could be presented would be of the order of 300 lines. The primary interest is in the higher spatial frequencies, probably in the neighborhood of 600 to 700 lines.

The approach used was to employ an electronic bar pattern generator together with a video blanking circuit to limit the bar length-to-width ratio and to move the monitors as close to the man as possible, 21" in this case. This approach eliminates the need for making display MTF corrections and permits the generation of higher spatial frequencies than would otherwise be possible.

The burst pattern generator can simultaneously generate patterns in 100-line increments from 100 to 1,000 lines. However, the monitor limited the highest spatial frequency to barely 800 lines per picture height. Two methods of psychophysical testing were used, the method of limits and the method of random SNR variation. In both cases, all of the patterns from 100 to 800 lines were simultaneously displayed. The SNR_D was cycled systematically from high-to-low and back to high for the method of limits. Three such cycles were performed per flight. Two hundred data points per man per condition was the usual number of data points taken per flight. The observer is requested to pick the highest spatial frequency that can be just barely discerned as a bar pattern. In the method of

random SNR variation, all of the patterns will be displayed as before but the SNR_D was randomly varied and the observer was again asked to state the highest frequency pattern he could just barely discern.

A typical experimenter's sheet is shown in Table 7 and in Table 8, the observer's data sheet is shown. Typically each observer used 5 data sheets per flight. The observer sheets were similar for the two experiments but the order of the dB settings was random in the one case.

Table 4-3 summarizes the total number of data points taken for the last four flights. In flight, three times more data was taken for the bar pattern experiment than was taken for the experiments with squares due to the setup.

The monitors were moved as close to the observer as was practical, 21" in this case, in order to permit the observers to discern the higher spatial frequencies. The monitor brightness with signal only was 2 f-L while with full noise, the brightness was 3 f-L, a slight reduction from the previous value as it was found in the lab tests that a higher contrast setting tended to bloom the high frequency pattern. An average of nearly 1,500 data points per flight were taken.

4.3 Analysis of Data

Before detailing the analysis of the data, the mathematical model used for calculating SNR_D for the bar patterns in the present case will be reviewed. The equation used is

$$SNR_D = \left(\frac{2t\varepsilon\Delta f_v}{\alpha}\right)^{\frac{1}{2}} \frac{1}{N} \left[\frac{\Delta V \text{ (from generator)}}{V_{rms} \text{ (noise)}}\right] . \qquad (5)$$

The height of each bar of the burst pattern is the same and equal to 1/20 the display height and thus $\varepsilon = (N/20)$.

The display MTF, which is a factor limiting observer performance, is ignored in the above calculation. However, we are concerned with the relative rather than the absolute

TABLE 7 EXPERIMENTERS SHEET

NAME _____ EXPERIMENT ____ DATE _____ TIME _____

V_{p-p} = _____ DETAIL #3 FLIGHT PATH _____

V_{rms} = _____ 11 and 11.5 ON LIGHT METER

#	db	#	db	#	db	#	db
1	5	26	29	51	5	76	29
2	6	27	28	52	6	77	28
3	7	28	27	53	7	78	27
4	8	29	26	54	8	79	26
5	9	30	25	55	9	80	25
6	10	31	24	56	10	81	24
7	11	32	23	57	11	82	23
8	12	33	22	58	12	83	22
9	13	34	21	59	13	84	21
10	14	35	20	60	14	85	20
11	15	36	19	61	15	86	19
12	16	37	18	62	16	87	18
13	17	38	17	63	17	88	17
14	18	39	16	64	18	89	16
15	19	40	15	65	19	90	15
16	20	41	14	66	20	91	14
17	21	42	13	67	21	92	13
18	22	43	12	68	22	93	12
19	23	44	11	69	23	94	11
20	24	45	10	70	24	95	10
21	25	46	9	71	25	96	9
22	26	47	8	72	26	97	8
23	27	48	7	73	27	98	7
24	28	49	6	74	28	99	6
25	29	50	5	75	29	100	5

TABLE 8 OBSERVER SHEET

OBSERVER SHEET - BAR PATTERN

MONITOR # _____

NAME _____ DATE _____ RASTER SIZE _____

#	RESOLUTION (HUNDREDS)	COMMENTS

TABLE 9 SUMMARY OF DATA COLLATED FOR BAR PATTERN EXPERIMENTS

Condition		Number of Data Points for Bar Patterns
Lab		2,600
Aircraft on Ground		800
Flight No. 5 -	Straight and Level	800*
(Method of Limits)	Straight and Level	440**
	2½ g Turns	160
Flight No. 6 -	Straight and Level	800
(Method of Limits)	2½ g Turns	100
	Rough Air	748
Flight No. 7 -	Straight and Level	800
(Random SNR)	2½ g Turns	120
	Rough Air	800
Flight No. 8 -	Straight and Level	400*
(Random SNR)	Straight and Level	400**
	2½ g Turns (Random SNR)	120
	2½ g Turns (Limits)	200
	TOTAL	9,288

* at start of flight

** at end of flight

thresholds as measured in a laboratory vs a flight environment. Display MTF should have the same effect in either environment. In the calibration data which were taken in the lab, three independent runs were made with three observers and in each case, the data was very consistent at low line numbers, but at 600 TVL/PH and above, there is a larger spread. In Table 10, the average SNR_D thresholds for the observers from the lab test are listed. The $\pm$ values are the $\pm$ 1 σ values and the average 1 σ value is 17% higher than the mean.

In Fig. 24, the data from the lab test and from the test in the airplane sitting on the ground are plotted. The average of the in-aircraft data is 25% higher than the lab data.

The first set of data for in-flight straight and level conditions using the bar patterns is shown in Fig. 25. Two sets of data were taken; the first, early in the flight and the second, late in the flight. It is interesting to notice that the data is virtually the same at the two portions of the flight for all but the highest spatial frequencies. The data point at 300 TVL/PH appears to be an anomaly. At 500 TVL/PH, the difference is about 18% whereas at 600 lines, the difference is 45%. A similar set of tests, early in and near the end of flight no. 8 for straight and level conditions was taken and these data are plotted in Fig. 26. A similar trend is noted in Fig. 26 as was seen in Fig. 25. Data taken late in the test for high spatial frequencies show somewhat higher thresholds, but the percentage changes are smaller, 13% and 11% for 520 and 600 TVL/PH respectively. It is concluded that the time the data is taken is of only a secondary importance for the observer thresholds.

Two other sets of straight and level data are shown in Fig. 27. One set which was taken by the method of limits on flight no. 6 and the other was taken using the method of random SNR variation as flight no. 7. As can be seen in Fig. 27, the two sets of data are very similar with the random SNR variation data being very slightly higher (on the average, 6% higher) but

TABLE 10 OBSERVER THRESHOLD SNR_{D-T} FOR BAR PATTERN RECOGNITION FROM LAB DATA

Observer	Spatial Frequency							
	101.3	216.6	300.0	410.5	519.9	600.0	709.1	821.1
WVU	2.62	1.91	1.95	2.30	2.72	3.43	4.83	7.94
DM	2.58	2.04	2.39	2.50	3.14	4.05	5.62	9.31
EJ	2.97	2.48	2.49	2.79	3.50	5.15	-	-
WS	3.87	2.89	2.99	3.05	3.47	4.11	6.16	-
MB	2.55	1.87	1.72	1.88	1.90	3.26	4.02	-
TS	2.90	2.23	2.16	2.43	2.28	3.78	5.35	-
* Average	2.92±.50	2.24±.39	2.28±.45	2.49±.40	2.84±.65	2.96±.67	5.20±.81	8.63±.97

* ± Values are ± 1 σ Values.

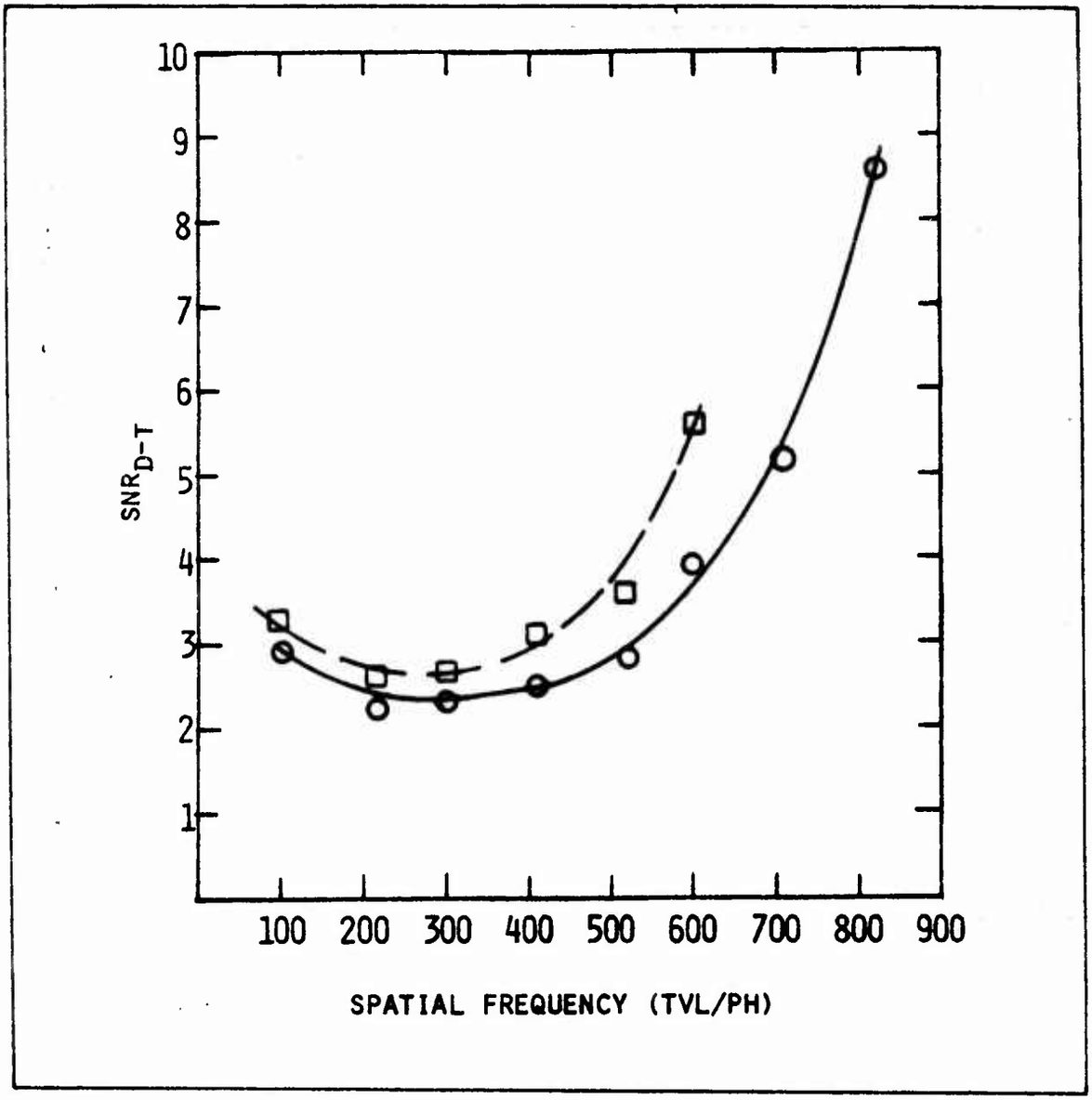

Figure 24 Threshold SNR_{D-T} for Bar Patterns of Constant Bar Length - o Average Lab Data and □ Data in Aircraft on Ground.

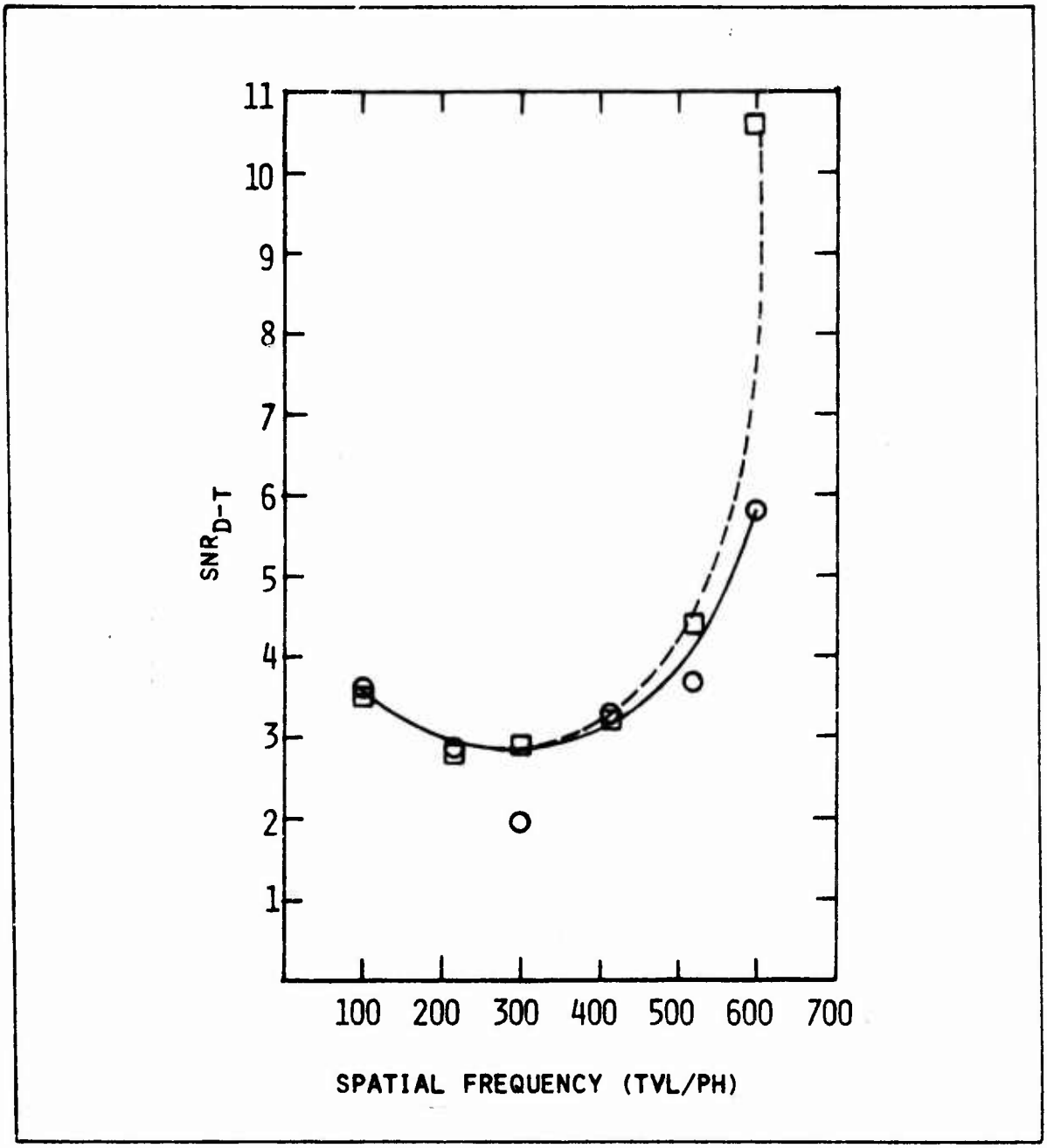

Figure 25 Threshold SNR_{D-T} vs Spatial Frequency for Flight No. 5 - o Data Taken Early in Flight and □ Data Taken Late in Flight. All Data for Straight and Level Flight - Method of Limits Used.

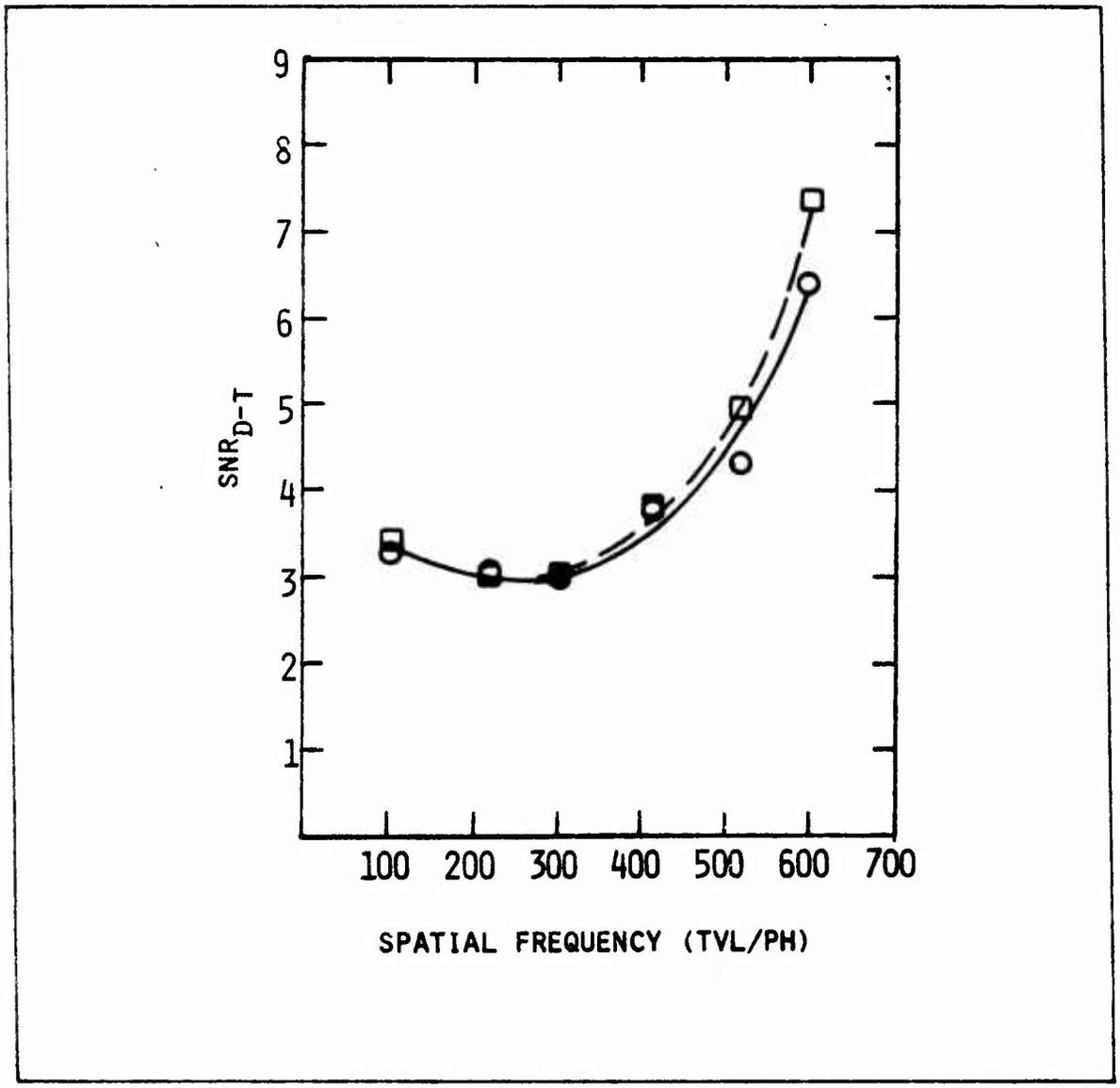

Figure 26 Threshold SNR_{D-T} vs Spatial Frequency for Flight No. 8 - o Data Taken Early in Flight and □ Data Taken Late in Flight. All Data for Straight and Level Conditions - Method of Random SNR Variation Used.

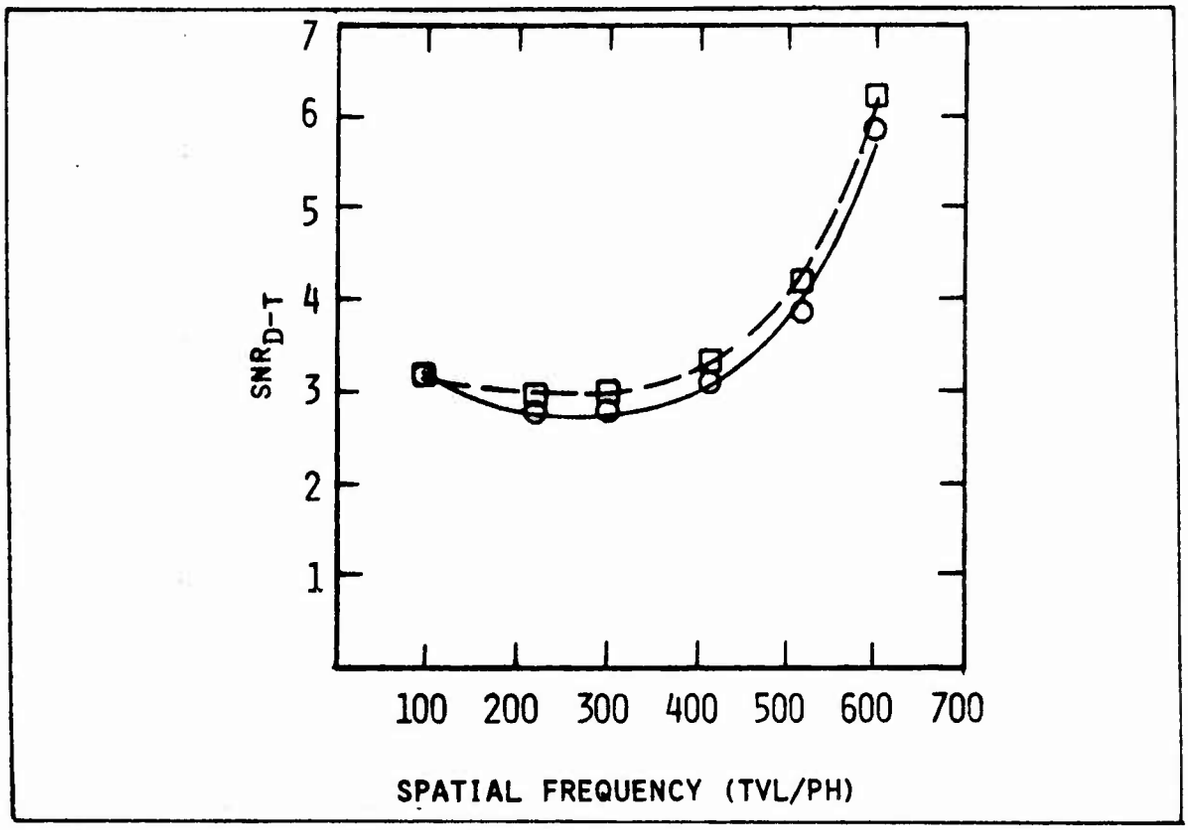

Figure 27 Threshold SNR_{D-T} vs Spatial Frequency for o Flight No. 6 (Method of Limits Used) and □ Flight No. 7 (Method of Random SNR Variation Used) for Straight and Level Flight Conditions.

the two sets of data are well within the expected experimental accuracy.

Finally in Fig. 28, the average of all of the data for straight and level conditions from flight nos. 5, 6, 7 and 8 are shown together with the $\pm$ 1 σ values on the data for the four flights. The 1 σ values are within 5 to 6% for the 100 and 217 TVL/PH and 15%, 9%, 11%, 26% for the other patterns from 300 to 600 respectively giving an average 1 σ variation of 12%.

Two sets of data were taken under turbulent conditions, one on flight no. 6 using the method of limits and one on flight no. 7 using random SNR settings. The average results for each flight are plotted in Fig. 29. For flight no. 6 the turbulence varied from $\pm$ 0.2 g to $\pm$ 0.6 g with occasional peaks to 1.2 g (approximate intervals were 3 sec in duration). For flight no. 7 similar turbulence was encountered ($\pm$ 0.2 g to $\pm$ 0.8 g with occasional peaks to 1.0 g). The time interval was not estimated. The data are virtually identical with that from flight no. 6 except at the 600 TVL/PH point. Using all of the data, the average + 1 σ is 8% larger than the mean value but excluding the 600 TVL/PH data, the average + 1 σ is only 4% larger than the mean.

The ratio of the SNR_{D-T} for average straight and level flight to the average SNR_{D-T} for turbulence conditions is plotted in Fig. 30 and as seen in the figure, a straight line fits the data points well.

Three different sets of data were taken while pulling 2½ g steep turns, two using random SNR settings and one using the method of limits for data collection over three different flights. The data is plotted in Fig. 31. The average + 1 σ variation in the data is 10%. The average 2½ g condition data is only 5% different from the average straight and level data and we conclude that the observer thresholds were only slightly influenced by the 2½ g constant g turns.

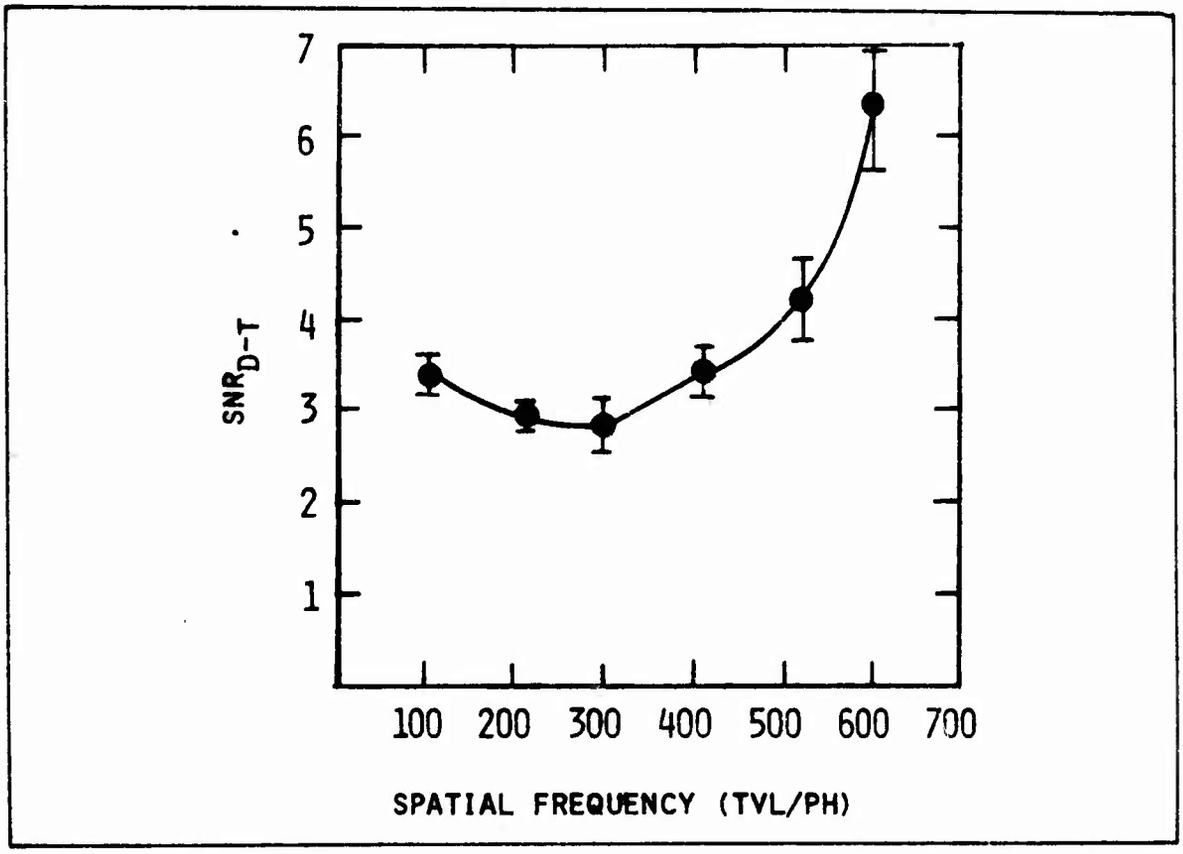

Figure 28 Average Threshold SNR_{D-T} for Bar Pattern Recognition Under Straight and Level Flight Conditions - $\pm$ 1 σ Limits (Φ).

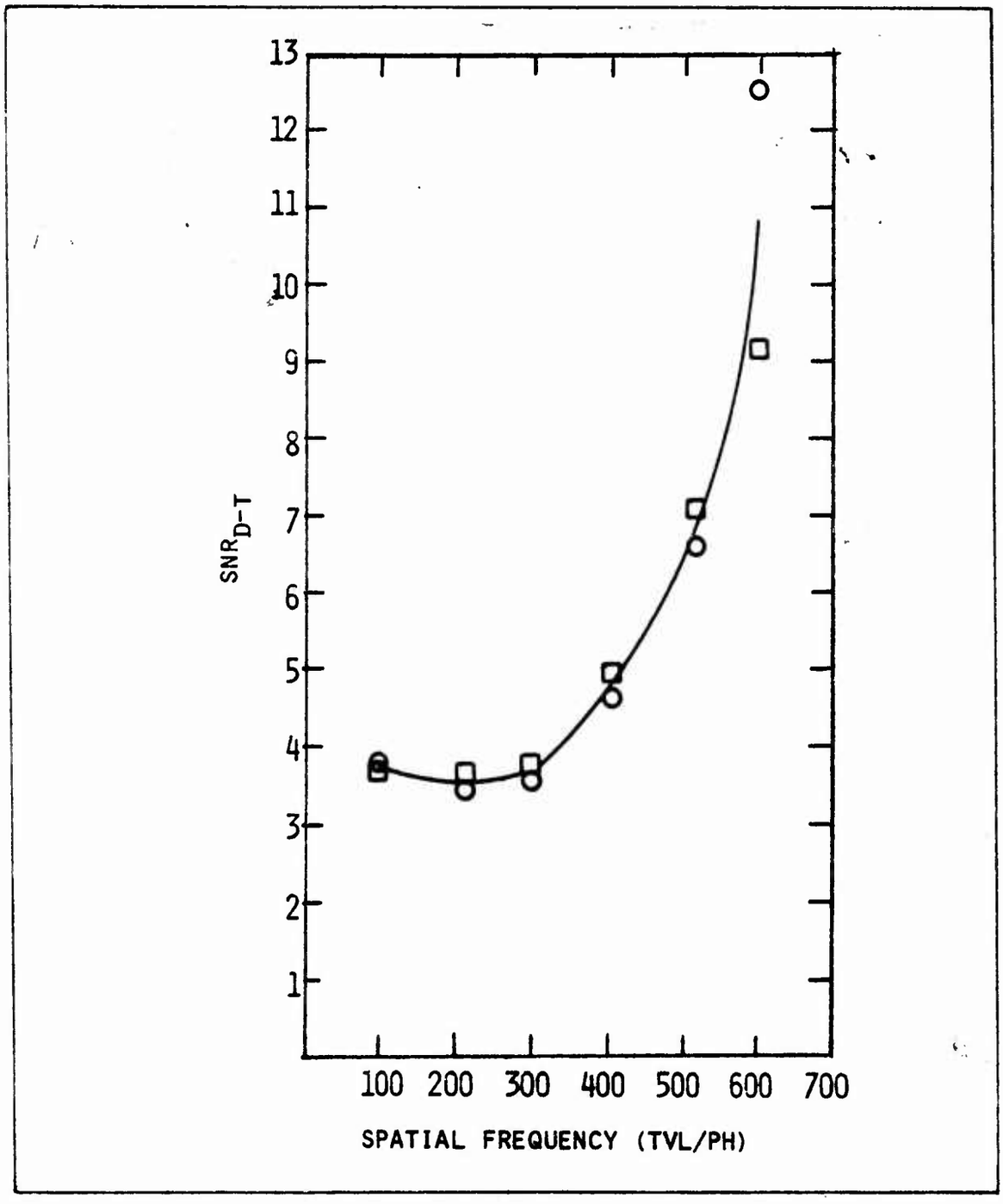

Figure 29 Threshold SNR_{D-T} for Bar Pattern Recognition Under Turbulent Conditions - o Method of Limits Flight No. 6, □ Random SNR Variation Flight No. 7, and (——) Average.

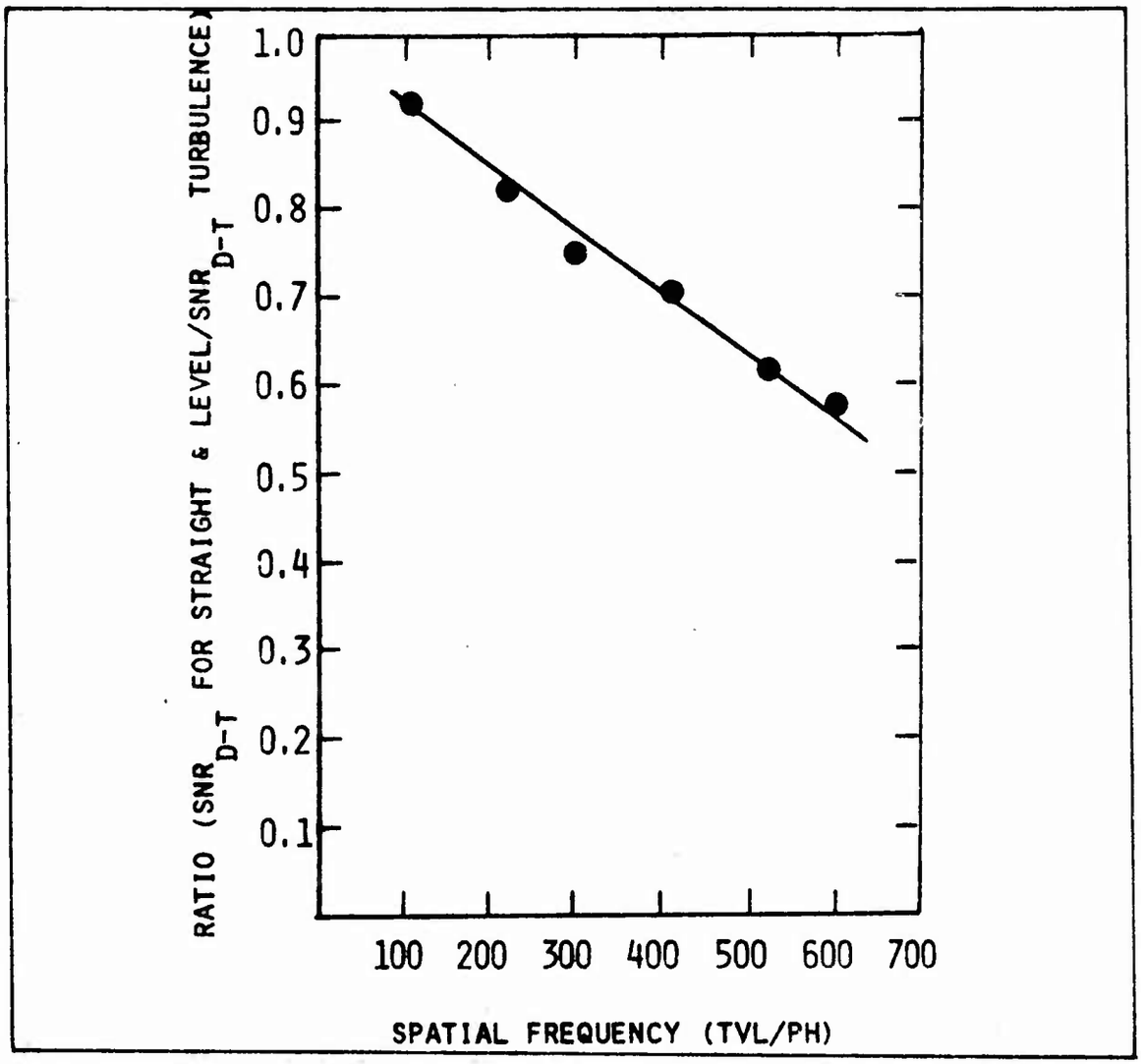

Figure 30 Ratio of SNR_{D-T} for Straight and Level Flight to the SNR_{D-T} for Turbulent Flight Conditions for Bar Pattern Recognition.

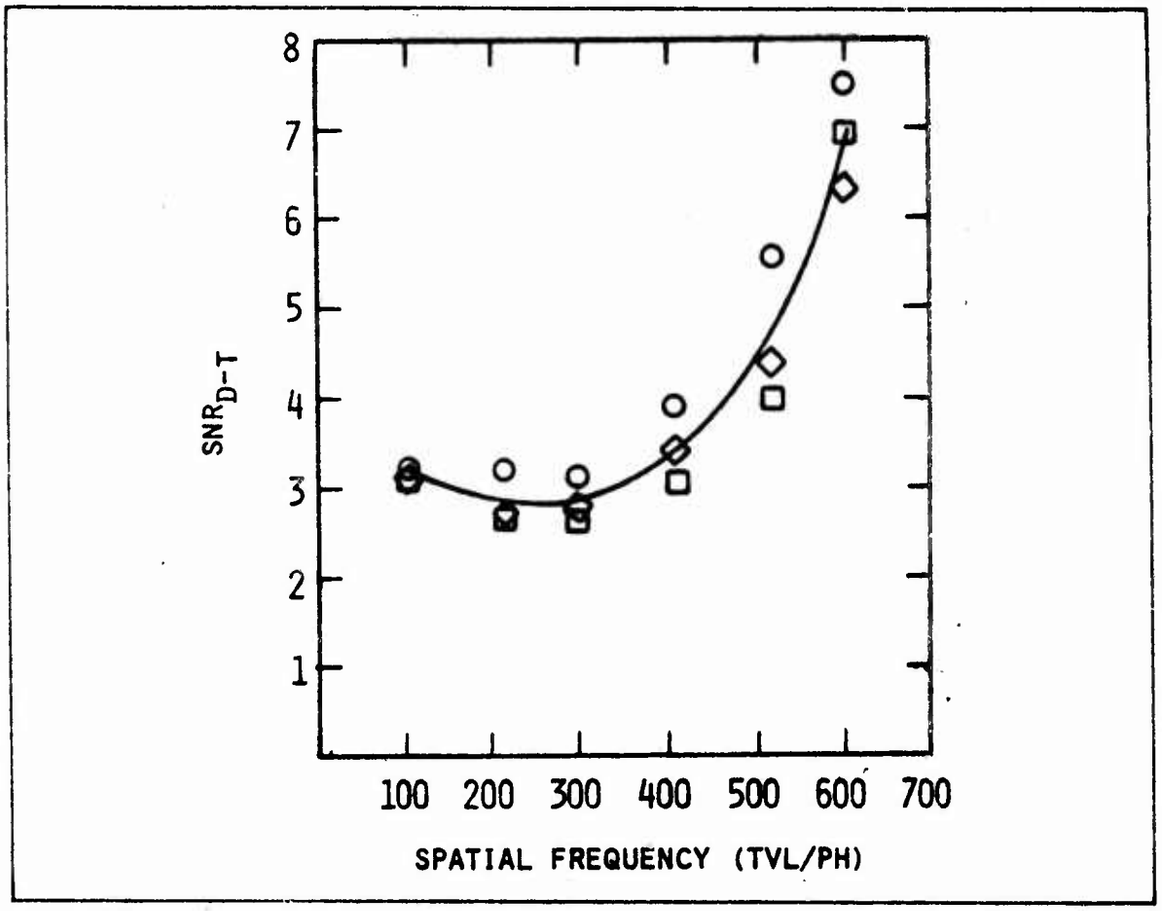

Figure 31 Threshold SNR_{D-T} as a Function of Spatial Frequency During 2½ g Steep Turns for Bar Pattern Recognition, o Random SNR Flight No. 7; □ Method of Limits Flight Nos. 5, 6, 8; ◇ Random db Flight No. 8; and (———) Composite Average.

Finally in Fig. 32, a composite plot is shown for the data, the aircraft on the ground, average straight and level flight, average 2½ g steep turns and the data for average turbulent conditions. The data for the aircraft on the ground, that for average straight and level flight and that for average 2½ g turns are very similar with the average 1 σ being 6% higher than the mean value. Separate curves were drawn through the data so that each set can easily be found.

4.4 Operator Comments

The observers thought that their performance was degraded with time but this was not borne out in the data. It was also noted that in rough air, the tasks seemed harder under - g impulses than + g impulses. Once into the constant 2½ g turns, the observers thought their performance was minimally influenced by the g's.

Although the data shows very little difference between using the method of limits or the random SNR variation method for data collection, there was a strong operator opinion which favored the random SNR variation experiment. In general, it was thought that the experiments, using random SNR settings were more interesting.

4.5 Vibration Data

As noted previously in section 2 of this report, accelerometer data was monitored in two ways: (1) accelerometers in the cabin area (on operator seats and table), and (2) in the pilot's compartment. Some difficulties were encountered with the cabin measurements due to equipment problems and the pilot's instrumentation was used as a reference. In cases where both instrumentations were available (flight no. 6, for example), there was good agreement. During straight and level flights and steady g's, there was relatively little g perturbations with the only significant dynamic g's occurring in the rough air flights. The g's for the rough air flights ranged from about

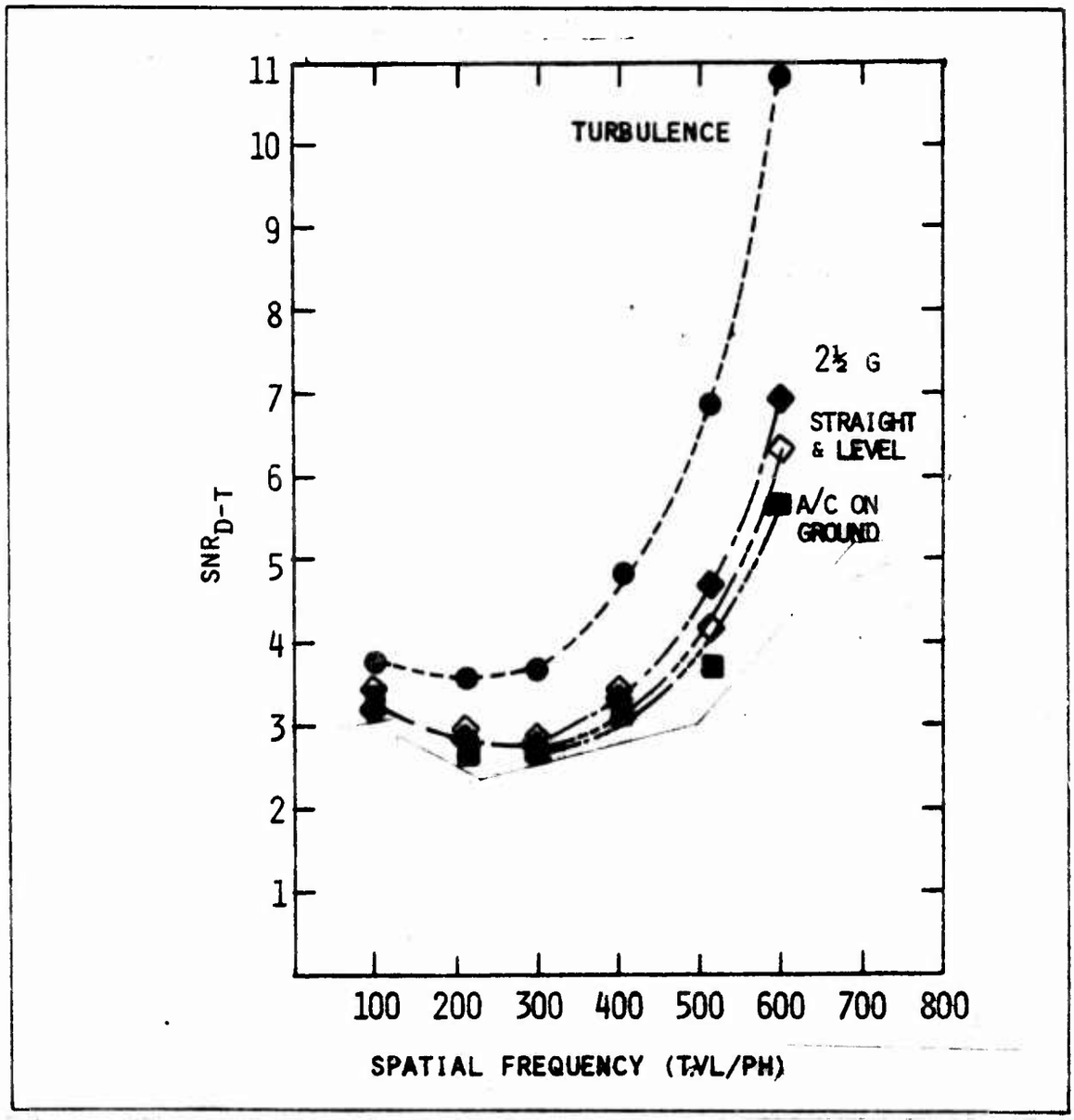

Figure 32 Composite Average Threshold SNR_{D-T} Data for Bar Pattern Recognition - ■ Aircraft on Ground, ◇ Straight and Level Flight, ◆ 2½ g Turns, and ● Turbulence.

0.2 to 0.6 with indications of local pulses of about 1 g. In the data analysis, the values obtained from the pilot's compartment accelerometer were used.

The AFAL attempted to analyze the vibration data and the results of their analysis are reported in Appendix A.

5.0 RECOMMENDED FOLLOW-ON EFFORTS

The effort reported herein represents one of the first-ever attempts to quantitatively measure the ability of observers to detect and discern image in a severe flight environment. While it is felt that a good start was made in this vital study area, cost and schedule constraints limited the quantity and variety of data which could be taken. As in any effort of this type, a certain amount of learning is involved but very little time was available to take advantage of the learning process. The test images employed were purposely limited to the simplest type for which a rather considerable data base of psychophysical experimentation exists. However, experiments using more realistic images are recommended. In this first step program, the fabrication of equipment racks and tables and the necessary modifications to the aircraft took rather more effort than was anticipated and did detract from the instrumentation effort. However, the racks and modifications are available for any future effort.

The recommended follow-on efforts are as follows:

a) Bar Pattern Tests - The principal g and turbulence effects on the observer are vertical in direction. In the first step effort only vertically oriented patterns were used. Further tests using inclined and/or horizontally oriented bars are indicated.

b) Real Image Tests - Perform psychophysical recognition and identification experiments using images of real tactical objects.

c) Search Task Tests - Perform detection, recognition and identification experiments using randomly located real objects in varigated backgrounds.

All of the above experiments are to be performed in the ground and flight environments. The follow-on effort should include a short study period to design the experiments and fabricate the means of image generation. Also, the instrumentation experiment operator controls should be upgraded to obtain better data and to ease the operator's work environment.

APPENDIX A

SUMMARY REPORT MOTION ANALYSIS, FLIR/ACTV AIRBORNE OPERATOR TEST PROGRAM

The following report is an analysis of the motion data which was performed and written by Mr. James McCormick of AFAL.

I. INTRODUCTION

A. Two FM recorded magnetic tapes were submitted by AFAL/RWI to AFAL/RWF for motion data analysis. The tapes contained motion data as recorded on Flights 6 and 7 of the FLIR/ACTV Airborne Operator Test Program. During these flights, the operator was tested for effectiveness during both calm and rough air flight modes. The purpose of this motion analysis is to determine the characteristics of the motion the operator encountered.

B. The following peculiarities were encountered and had to be considered before useful data could be obtained.

1. In the normal process of 14 channel magnetic tape recordings, two magnetic heads are used, 7 channels per head. According to IRIG (Inter-Range Instrumentation Group) standards, the odd numbered channels are spaced 1.50 inches in front of the even numbered channels. In the playback mode, the same arrangement restores the proper phase relationship between the even and odd channels. For the tapes analyzed, the standard playback operation put the odd channels an effective 0.2 seconds (3 inches) ahead of the even channels relative to the 15"/sec tape speed, concluding that the placement of the magnetic heads was reversed for the record mode.

2. The tape speed, during the record mode, was very irregular as was determined by the presence of noise signals common in amplitude and frequency to all channels. Because of the

presumably non-standard record magnetic head placement there was a 0.2 second time delay between the noise signals of the odd and the even numbered channels.

3. The channel designations, relative to sensor location in the aircraft, were confused. The original designation provided to us, was as per Table 11. Observance of the tape output showed IRIG time on Channel 1. Communication with the contractor verified Channel 1 as the IRIG time channel, but actual channel designation for the motion data was not known. Further observance of the data on the tape revealed Channels 2, 3, and 7 contained no motion data but did contain noise outputs because of the irregular tape record speed as before mentioned.

4. The sensitivity of Channels 4, 5, and 6 seemed about ten times that of Channels 9, 10, 11, and 12, and two times that of Channels 8 and 14. Also Channel 13 seemed alive but very erratic. This would give 10 active Channels but only 9 were designated as per Table 11. Channel 14 was also, at times, erratic and was void of the higher frequency data as associated with the other data channels. Presumably the accelerometer of Channel 14 was not secured tightly and the signal of Channel 13 is from a loose accelerometer or from another type sensor. The sensitivity per the contractor provided information, was 0.95 g peak per 1.0 volt RMS.

II. PROCEDURES

A. The flight tapes were re-recorded to eliminate the effect of the irregular flight tapes recording speed. Since Channels 2 and

3 appeared to have only this noise and no actual data, elimination of the noise from the data channels was achieved by electronically subtracting the noise on Channel 2 from all of the even numbered channels and the noise on Channel 3 from all of the odd numbered channels. A sample of this noise elimination is shown in Figure 33. As mentioned before, the channel sensitivities seemed to be different. From past experience in aircraft motion analysis, it seems the levels determined for Channels 4, 5, and 6 would be most nearly correct. For these channels, the overall amplitude averaged about 0.15 g to 0.25 g for the calm air mode and 0.3 g to 0.5 g for the rough air mode. All of the data presented in this analysis is given relative to the contractor provided sensitivity specification of 0.95 g peak per 1.0 volts RMS.

B. An analog recording was then made of each re-recorded data channel of each flight. Samples of these records are shown in Figures 34 and 35 and show the overall acceleration levels of the calm and the rough air modes respectively. These recordings were used to derive the Amplitude-Time plots of Figures 36 and 37. Short term or transient amplitudes were not considered and the levels are hence indicative of amplitude versus time trends only, and not meant to be precise. The tendency of the amplitude to periodically oscillate between two amplitude levels may be due to the aircraft periodically reversing its flight direction. The direction of flight, relative to the air currents, can cause significant changes in the motion response. These plots show the overall acceleration amplitudes increased by a factor of about 2 between the calm and the rough air modes.

C. Analog traces were also made at faster paper record speeds to better identify frequency components. Samples of these records are shown in Figures 38 and 39. From these records, predominant frequency bands were determined and band pass filters were then used to record the motion amplitudes within restricted pass bands. This was accomplished for samples of both the calm and the rough air modes and plotted as per Figures 40 to 42. These curves are only valid at the frequencies indicated by the data points. The data points are connected together only to preserve channel identification. Figures 40 and 41 are for the rough air mode and Figure 42 the calm air mode. Only two data channels are shown in Figure 42, but the others were similar in response. The low frequency amplitudes (frequencies below 60 Hz) for the rough air mode are shown to be up to 10 times the amplitudes during the calm air mode. In contrast, the high frequency amplitudes are about the same for both flight modes.

D. Conclusions

1. The most significant difference between the calm and rough air modes is in the low frequency motions. Below 60 Hz the rough air motion is up to 10 times the amplitudes of the calm air mode. Consequently, the operator effectiveness test is essentially one relative to low frequency motion.

2. Acceleration amplitudes below 60 Hz are quite low during the calm air mode. Even though these motions are increased

up to a factor of 10 for the rough air mode, the overall increase between the calm and rough air, considering all frequencies, is only a factor of about 3. The frequencies above 60 Hz are higher for the calm air and are not increased significantly for the rough air. The overall average acceleration is estimated to be about 0.15 g to 0.3 g for the calm air and up to 0.45 g for the rough air. It should be noted, however, that if these acceleration factors (g) were converted to velocity factors ("/sec), then the overall amplitude relationship between the calm and rough air modes would then more nearly be a factor of about 10 instead of 3. Converting to velocity from acceleration is an integration process which emphasizes the low frequency amplitudes.

3. Figures 36 and 37 should be especially useful for relating the operator effectiveness to particular times during the flights.

4. Since there was no rate sensor datum recorded, no relationship to the high "G" turn aircraft mode could be defined. However, these motions should have been fairly well defined during the flight and a direct relation to these motions made at that time.

TABLE 11 FLIGHT TEST CHANNEL DESIGNATION

Channel Number	Acceleraometer Location
1	Rear Left Seat - Vertical
2	Rear Left Seat - Sideways
3	Rear Left Seat - Fore and Aft
4	Front Right Seat - Vertical
5	Front Right Seat - Sideways
6	Front Right Seat - Fore and Aft
7	
8	Table - Sideways
9	
10	Table - Vertical
11	Table - Fore and Aft
12	
13	
14	

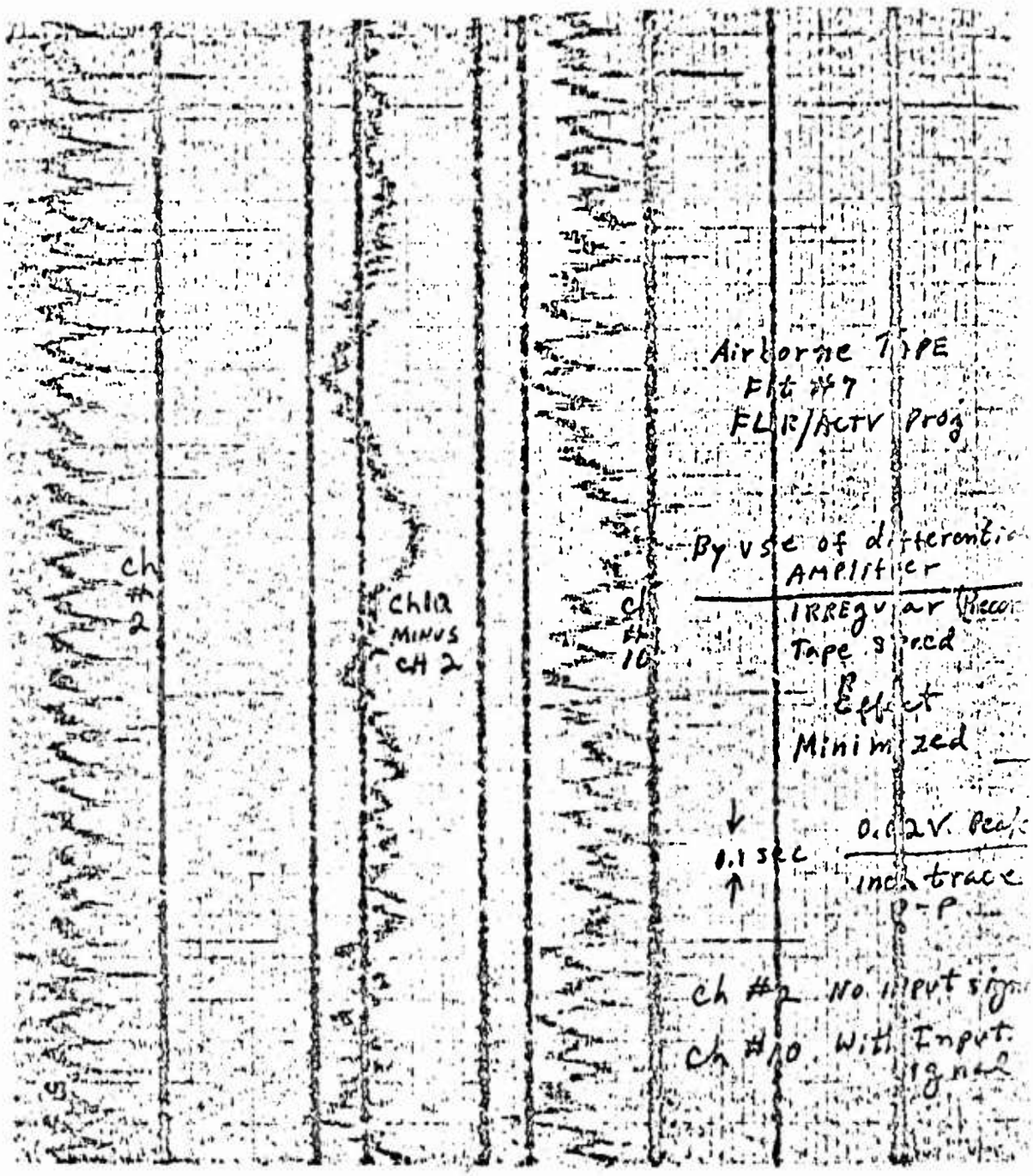

Figure 33 Elimination of Irregular Tape Record Speed Effects.

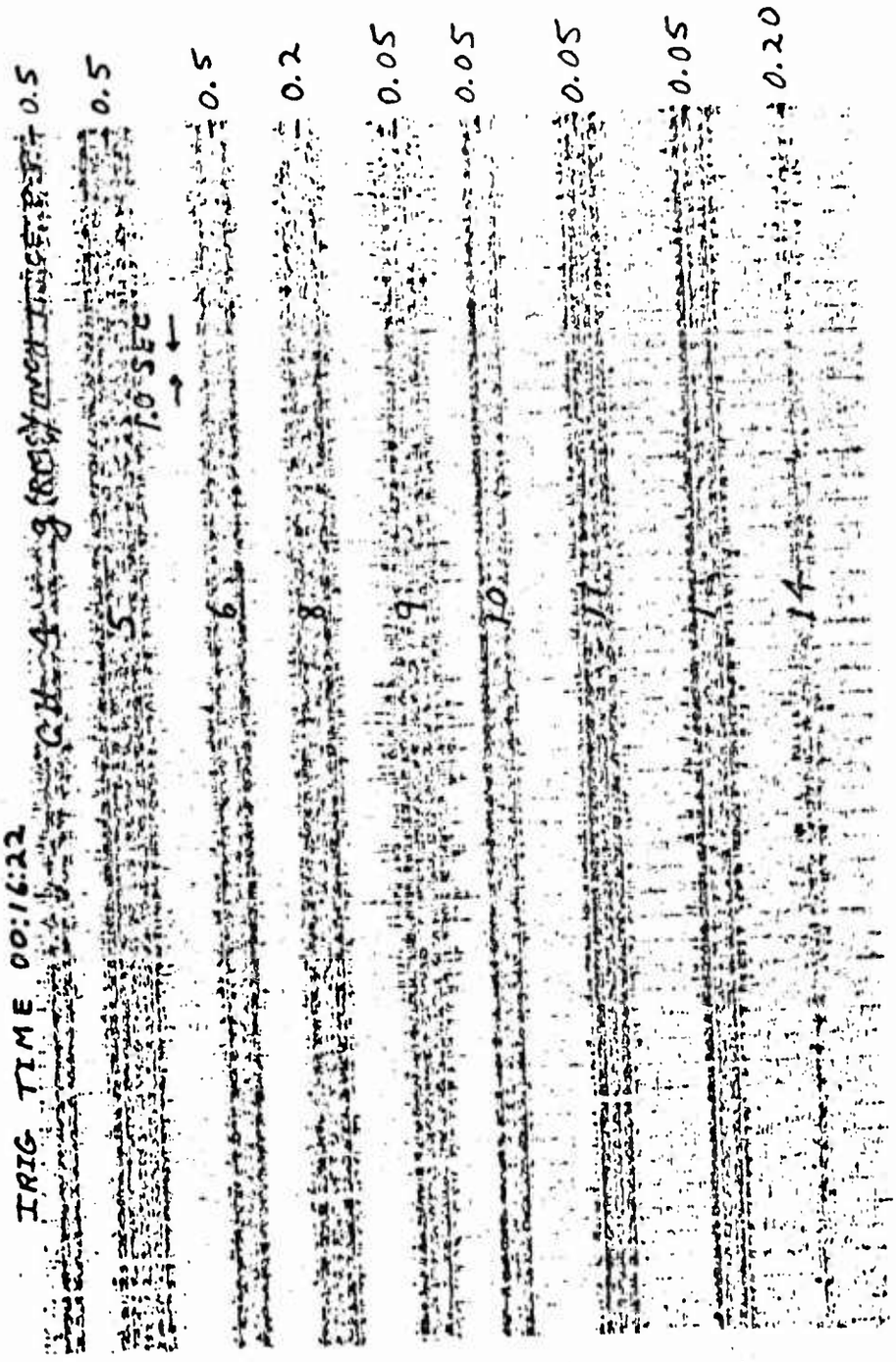

Figure 34 Calm Flight Mode - Slow Paper Speed - Illustrating Overall Acceleration Levels (Flight No. 6).

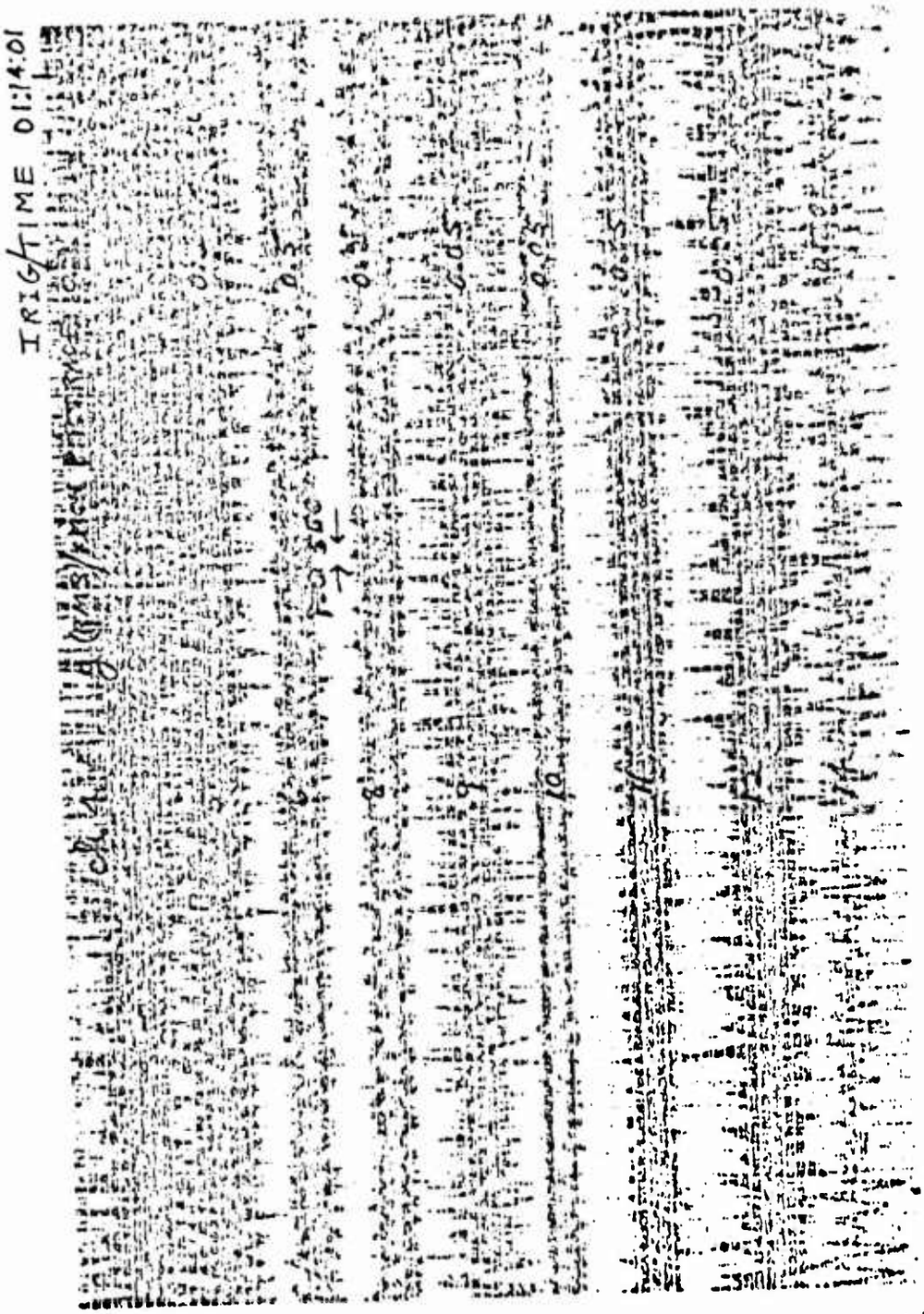

Figure 35 Rough Flight Mode - Slow Paper Speed - Illustrating Overall Acceleration Levels (Flight No. 6).

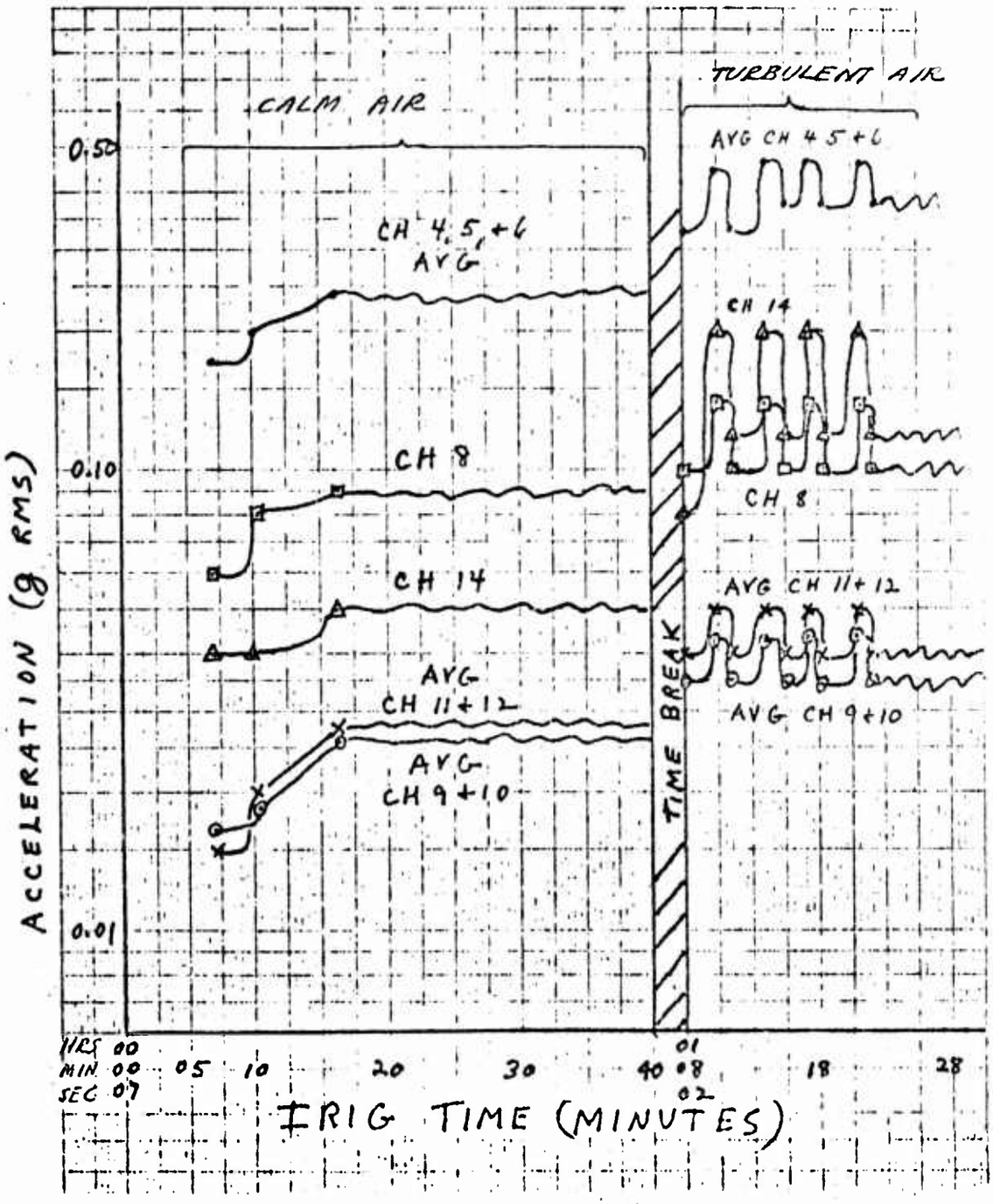

Figure 36 Average Overall Acceleration Levels (Flight No. 6) Relative to Flight Time Log.

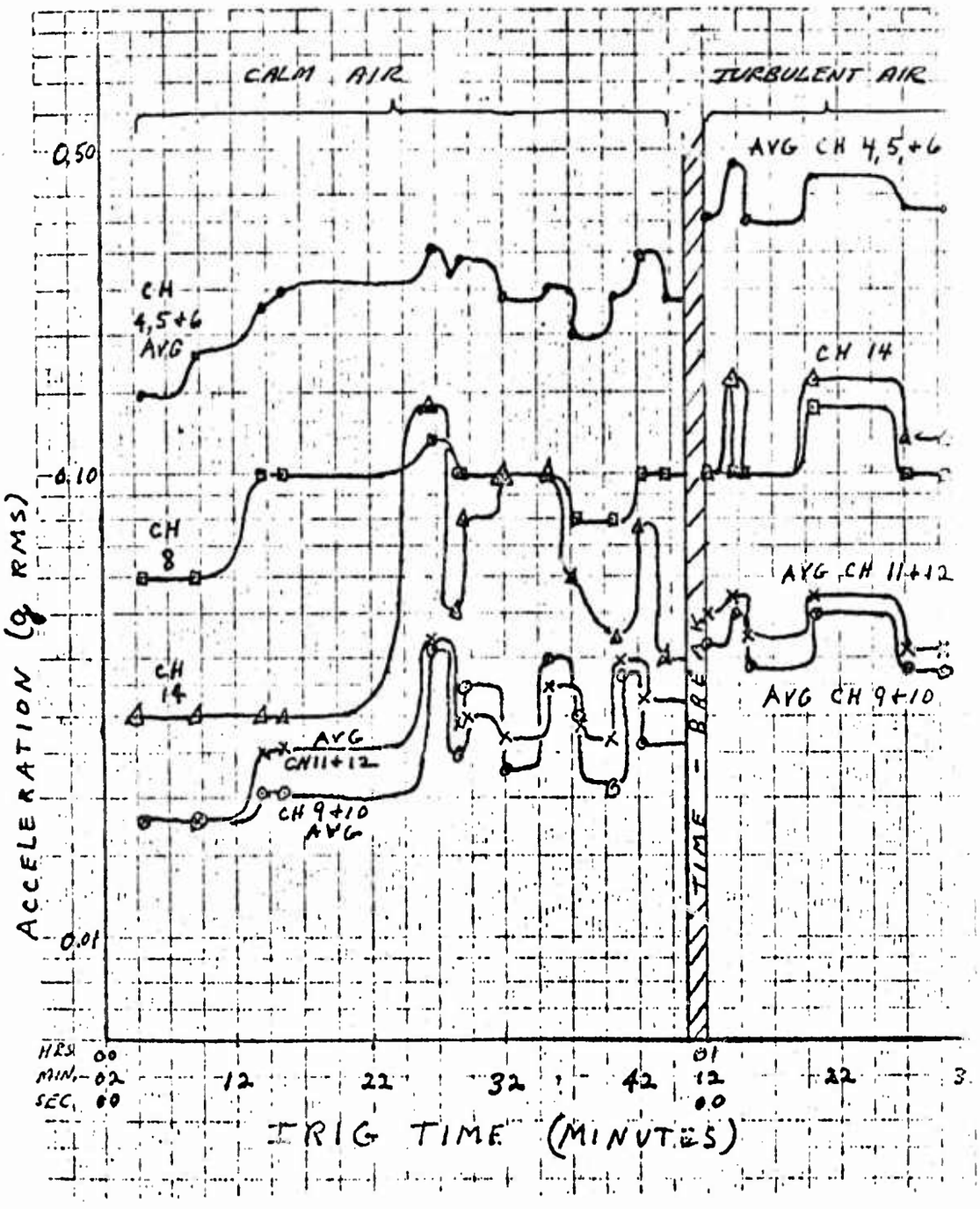

Figure 37 Average Overall Acceleration Levels (Flight No. 7) Relative to Flight Time Log.

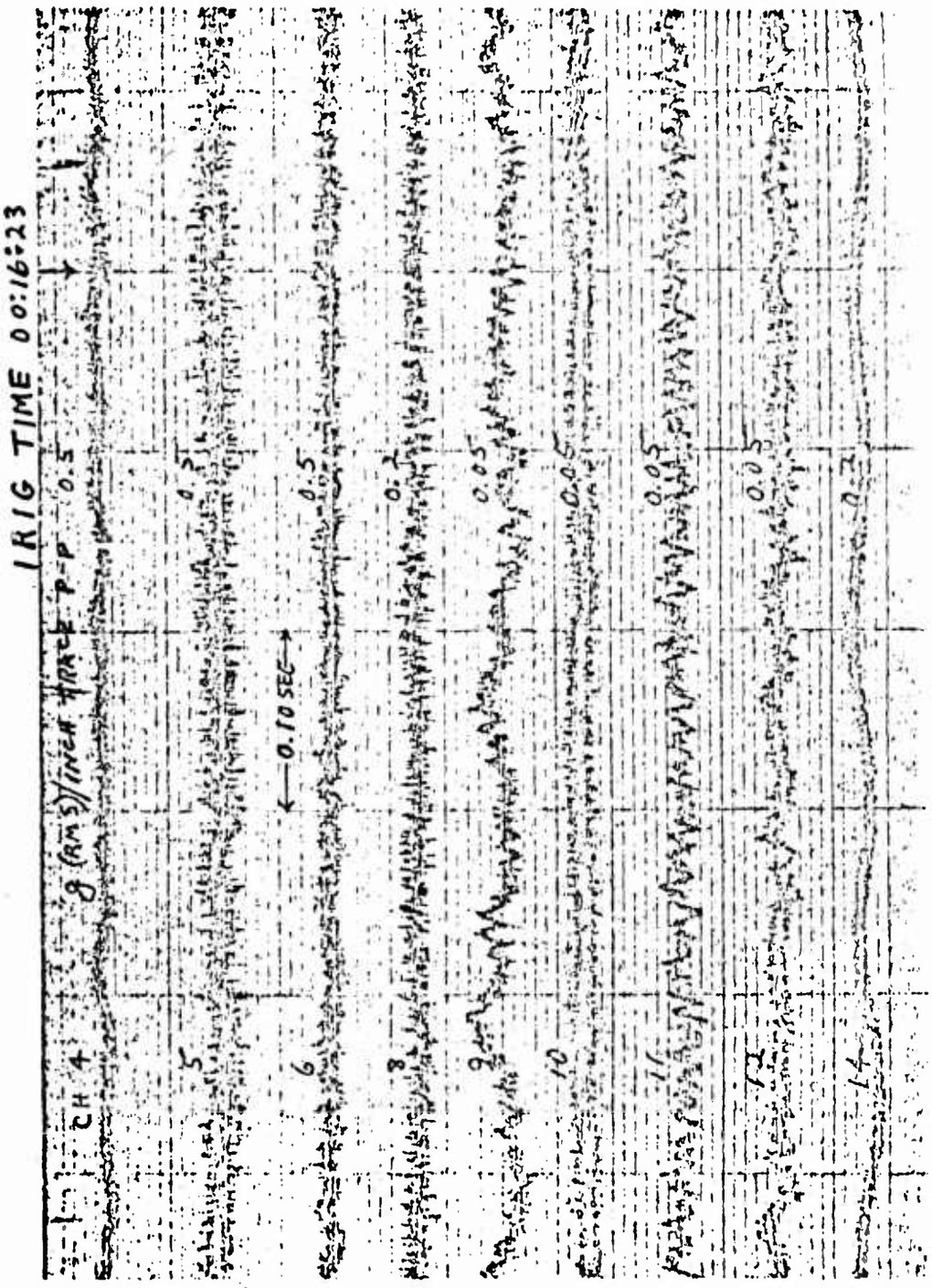

Figure 38 Calm Flight Mode - Fast Paper Speed - Illustrating Frequency Components of Motion (Flight No. 6).

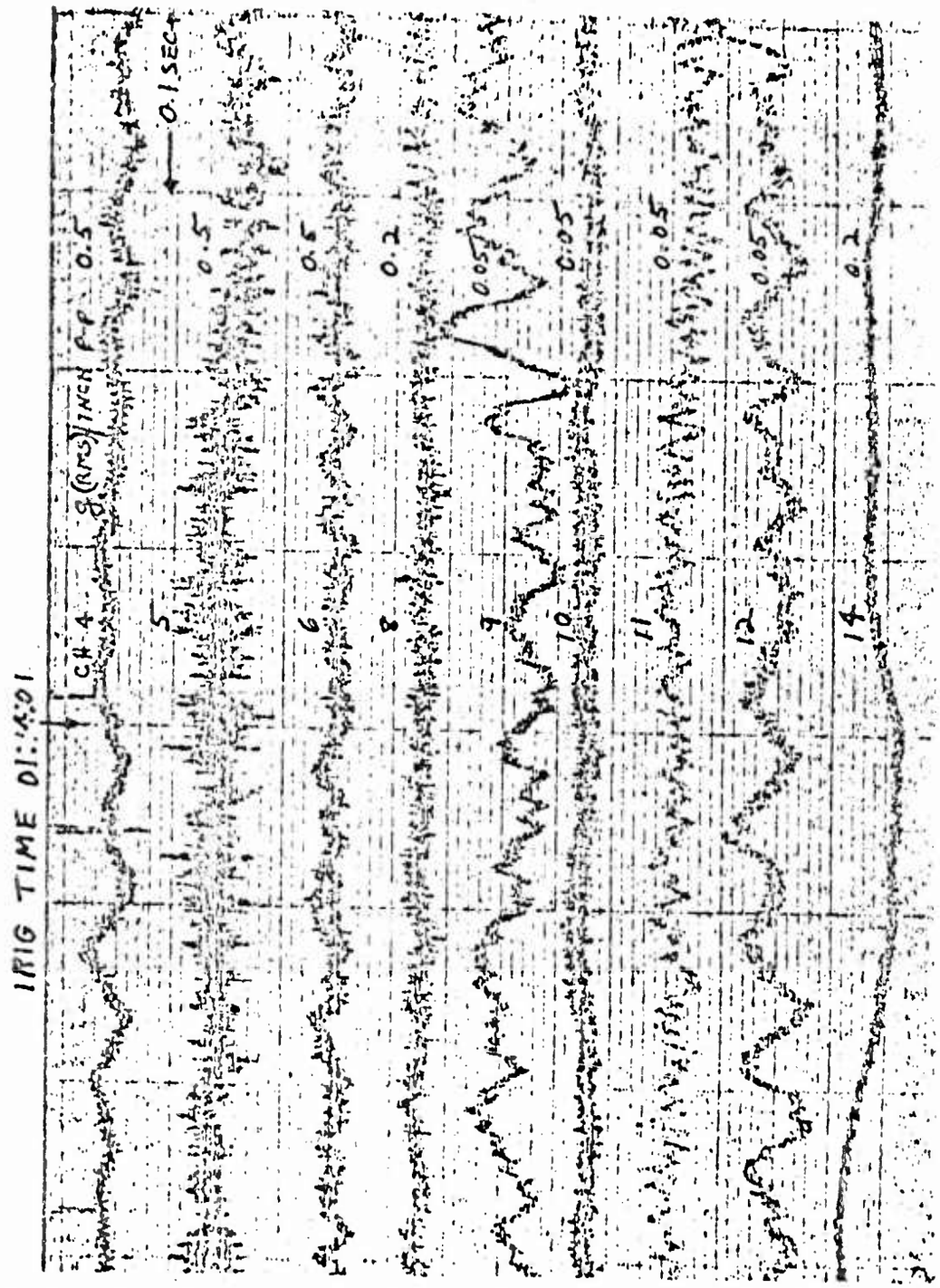

Figure 39 Rough Flight Mode - Fast Paper Speed - Illustrating Frequency Components of Motion (Flight No. 6).

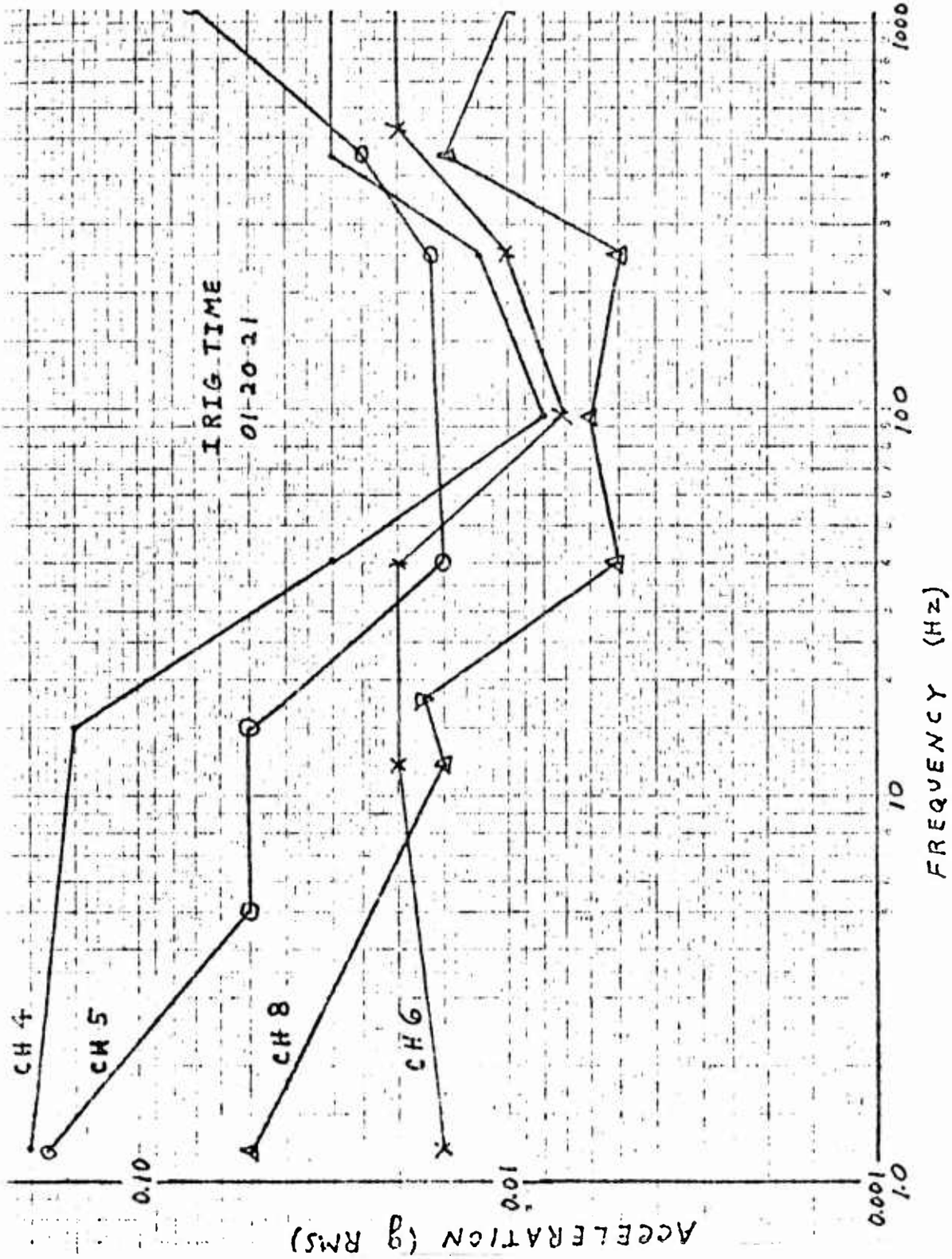

Figure 40 Rough Flight Mode (Flight No. 7) - Average Acceleration Amplitude vs Amplitude vs Frequency - Channels 4, 5, 6, and 8.

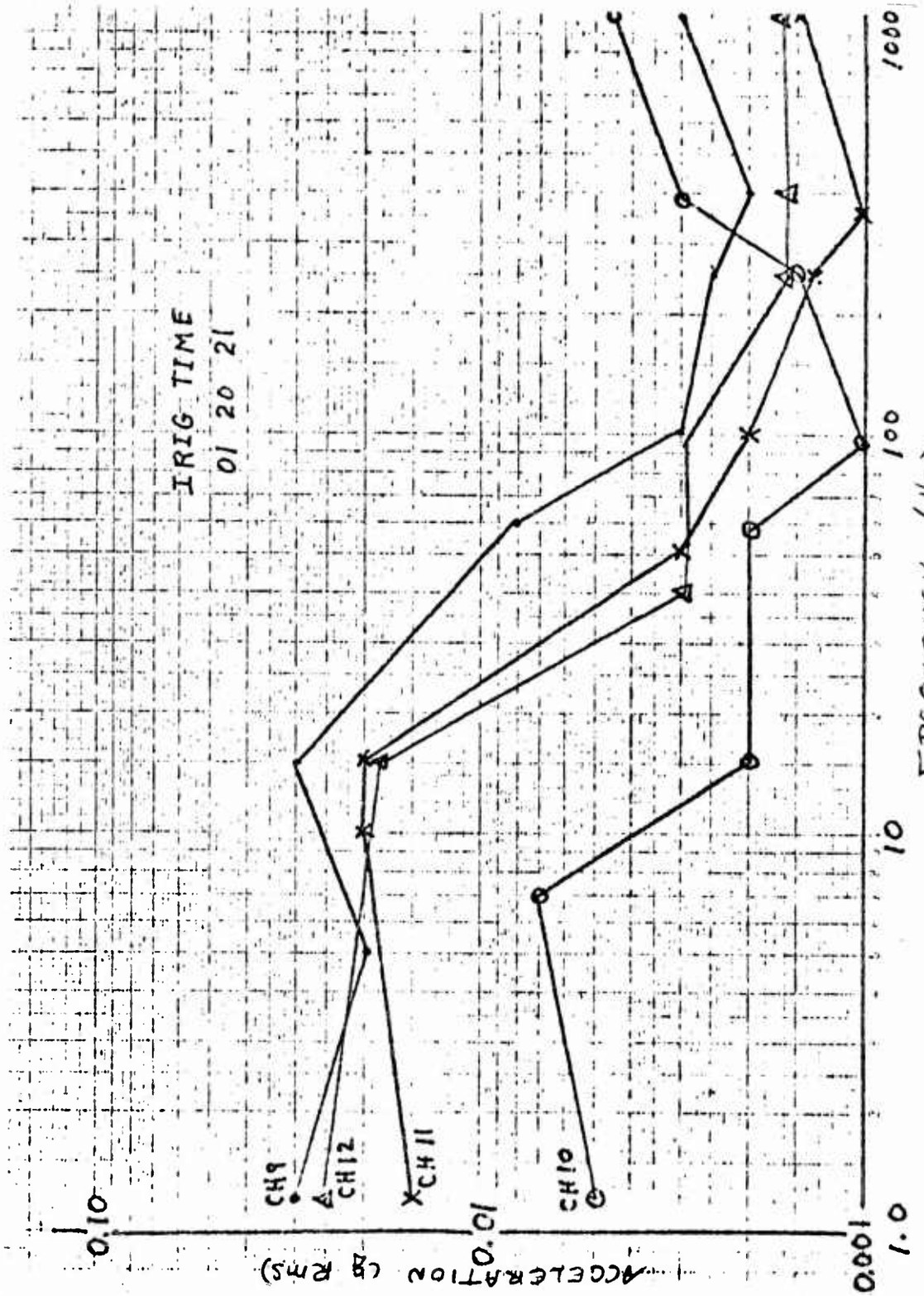

Figure 41 Rough Flight Mode (Flight No. 7) - Average Acceleration Amplitude vs Frequency - Channels 9, 10, 11, and 12.

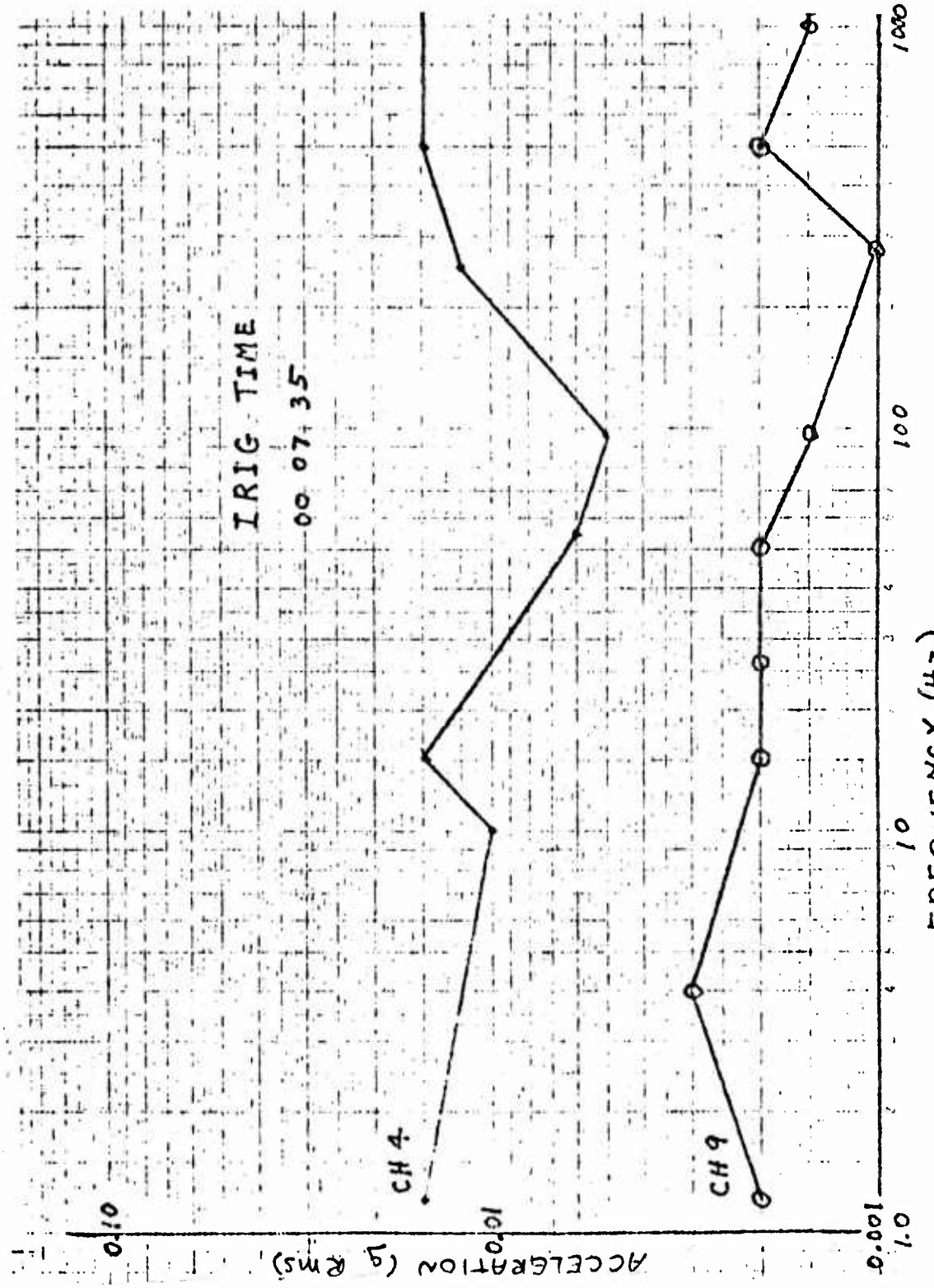

Figure 42 Calm Flight Mode (Flight No. 7) - Average Acceleration Amplitude vs Frequency - Channels 4 and 9.